ISSN 1813-3290, http://www.revist.ci

NON-PLANAR CRACKS IN UNIFORM MOTION UNDER GENERAL LOADING

P. N. B. ANONGBA

Université F. H. B. de Cocody, U. F. R. Sciences des Structures de la Matière et de Technologie, 22 BP 582 Abidjan 22, Côte d'Ivoire

(reçu le 07 Septembre 2020 ; accepté le 11 Décembre 2020)

* Correspondance, e-mail : *anongba@gmail.com*

ABSTRACT

Non-planar x_2x_3-plane-fronted cracks with arbitrary shapes, inside an infinitely extended isotropic elastic medium, whose finite lengths along the x_1-direction increase at a constant velocity $2v$, are the subject of the present study. The mixed mode $I+II+III$ loading as well as traction-free crack face condition are assumed, with loadings σ_{22}^a, σ_{21}^a, σ_{23}^a along x_2, x_1 and x_3 directions (respectively). The crack front in the x_2x_3-plane located at spatial position x_1 has an average elevation $h=h(x_1)$ from Ox_1x_3 and fluctuates weakly there in the form $\xi = \xi(x_1, x_3)$. The crack is represented by a continuous distribution of three types J ($J=I$, II and III) of dislocation having the shape of the crack front. Their Burgers vectors $\boldsymbol{b}_J$ are directed along the applied tension and shears, respectively. Explicit expressions of the dislocation elastic fields (displacement and stress) are first given. Then distribution functions D_J of straight dislocations, corresponding to a planar crack π_0 tilted (around Ox_3) by angle θ_0 from Ox_1x_3, are given. Adopting these D_J, we propose explicit expressions of the crack-tip stresses and crack extension force G per unit length of the crack front. The analysis is subsequently applied to a simple special non-planar crack having a crack-front composed by two types (A and B) of straight segments inclined by angles ϕ_A and ϕ_B from the x_3-direction; the average fracture surface is plane π_0. Expressions $< G >$ of G averaged over the length of the oscillatory crack-front are displayed. Two types of segmentation under dominant mode I loading are shown: (i) Strong segmentation ($\phi_A = \phi_B = 70°$). At $\theta_0 = 54°$, $< G >$ as a function of v displays a maximum $<G>_{max}$ larger than G_0, the corresponding value of the crack extension force when the moving crack is planar in Ox_1x_3. This indicates that a steady motion along x_1 of this non-planar crack configuration may occur under load in dynamic fracture experiments. (ii)

Flat fracture surface with isolated segmentations ($\phi_A = 0.1°$, $\phi_B = 88°$). At $\theta_0 = 35°$, $< G >$ (v) displays a maximum larger than G_0 indicating again that this configuration can propagate steadily. These configurations explain crack branching observed in brittle materials.

Keywords : *fracture mechanics, linear elasticity, crack propagation and arrest, dislocations, crack extension force.*

RÉSUMÉ

Fissure non plane en mouvement uniforme sous sollicitation extérieure arbitraire

Des fissures, ayant une forme non plane arbitraire avec un front plan parallèle à x_2x_3 dont les longueurs suivant la direction x_1 augmentent à vitesse constante 2v, font l'objet de la présente étude ; le milieu de propagation est isotrope, élastique et infiniment étendu. Le mode de sollicitation est mixte *I+II+III* avec des contraintes σ_{22}^a, σ_{21}^a, σ_{23}^a appliquées le long des directions x_2, x_1 and x_3 (respectivement). On applique la condition que les forces sur les faces de la fissure sont nulles. Le front de fissure dans le plan x_2x_3 situé en x_1 a une côte moyenne $h = h(x_1)$ par rapport à Ox_1x_3 et ondule faiblement sous la forme $\xi = \xi(x_1, x_3)$ à cette hauteur. La fissure est représentée par une distribution continue de trois types *J (J=I, II* et *III)* de dislocation ayant la forme du front de fissure. Leur vecteur de Burgers $\boldsymbol{b}_J$ sont dirigés le long de la tension et des cisaillements appliqués, respectivement. Des expressions explicites des champs élastiques (déplacement et contrainte) des dislocations sont d'abord calculées. Ensuite, des fonctions de distribution D_J de dislocations droites, correspondant à une fissure plane π_0 tiltée (autour de Ox_3) d'un angle θ_0 à partir de Ox_1x_3 sont données. En adoptant ces D_J, nous proposons des expressions explicites des contraintes en tête de fissure et de la force d'extension G de la fissure par unité de longueur du front de fissure. L'analyse est par la suite appliquée à une forme spéciale de fissure non plane ayant un front constitué de deux types (*A* et *B*) de segment droit inclinés des angles ϕ_A and ϕ_B par rapport à la direction x_3 ; la surface de rupture moyenne est le plan π_0. Des expressions $< G >$ de G moyennée sur la longueur du front oscillant de la fissure sont données. Deux types de segmentation, sous un mode *I* de sollicitation en tension dominant, sont exhibés : *(i)* Forte segmentation ($\phi_A = \phi_B = 70°$). Pour $\theta_0 = 54°$, $< G >$ en fonction de v présente un maximum $< G >_{max}$ plus élevé que G_0, la valeur correspondante de la force d'extension de la fissure plane voyageant dans le plan Ox_1x_3. Ceci indique qu'un mouvement stationnaire de cette configuration

de fissure non plane peut se développer sous charge dans des essais de fracture. *(ii)* Surface de fracture plate avec des segmentations isolées (ϕ_A = 0.1°, ϕ_B = 88°). Pour θ_0 = 35°, < G >(v) exhibe un maximum plus grand que G_0 indiquant de nouveau que cette deuxième configuration de fissure peut se propager à vitesse stationnaire sous tension dominant. Ces configurations de fissure expliquent bien la ramification des fissures observée dans des matériaux fragiles.

Mots-clés : *mécanique de la rupture, élasticité linéaire, propagation et arrêt de fissure, dislocation, force d'extension de fissure.*

I - INTRODUCTION

This work is a first attempt to analyse non-planar cracks in motion in an elastic medium by using explicit expressions of the elastic fields (displacement and stress) of moving crack dislocations. In previous studies [1 - 7], non-planar cracks are static with their planar front developed in a Fourier series. They are described by a continuous superposition of sinusoidal dislocations. We shall provide a generalization of this modelling by allowing the crack front plane to move uniformly at a velocity v in the subsonic velocity regime ($v < c_t$, the velocity of transverse sound waves). We consider an isotropic, elastic and infinitely extended medium to which we attach a Cartesian system x_i. It consists of a non-planar crack of finite extensions along x_1 and x_2 and infinite in the x_3- direction. Initially the crack is static and extends along x_1 from x_1= $-a$ to a. It spreads at any x_1- spatial position in the x_2x_3- plane in the form of a Fourier series

$$f = \sum_n \left(\xi_n \sin \kappa_n x_3 + \delta_n \cos \kappa_n x_3\right) + h(x_1) \equiv \xi(x_1, x_3) + h(x_1) \tag{1}$$

Here n is a positive integer; h, ξ_n, δ_n and κ_n are real that are $x_1 -$dependent. The static case has been treated in [5, 6]. ***Figure 1*** gives an illustration of the crack front. At a given time taken as t= 0 and under general loading, it starts moving at constant velocity v in the x_1- direction. Its extension after incremental time t is given by $|x_1| \le c = a + vt$. In addition to moving uniformly along x_1, we demand that the crack faces be free from any traction. The loadings correspond to mixed mode I+II+III with tension σ_{22}^a and shears σ_{21}^a and σ_{23}^a applied at infinity. The treatment also includes normal induced stresses σ_{11}^a = $\sigma_{33}^a = -\nu\sigma_{22}^a$ originating from the Poisson's effect. The crack is represented by a continuous distribution of three types of infinitesimal moving dislocations J *(J=I, II and III)* having the shape f (1) with Burgers vectors $\vec{b}_I = (0, b, 0)$,

$\vec{b}_{II} = (b, 0, 0)$ and $\vec{b}_{III} = (0, 0, b)$,respectively. Types *I* and *II* are of edge character on average and type *III* screw.

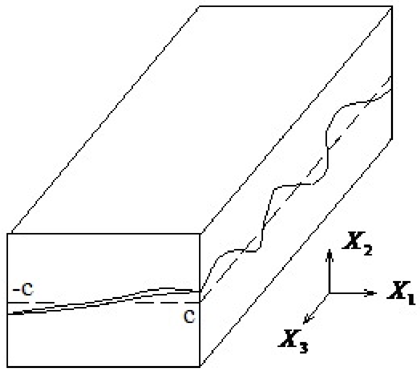

Figure 1 : *Illustration of the crack front that lies in x_2x_3 in the form f* (1). *Mixed mode I+II+III loading is assumed with loadings* σ_{22}^a , σ_{21}^a , σ_{23}^a *along x_2, x_1 and x_3 directions (respectively)*

Dislocation distributions D_J (*J*= *I* , *II* and III) are defined such that $D_J(x_1^{'})dx_1^{'}$ represents the number of dislocations *J* in the infinitesimal x_1 – interval $dx_1^{'}$ located about the x_1 – spatial position $x_1^{'}$. The elastic fields (displacement $\vec{u}^{(J)}$ and stress $(\sigma)^{(J)}$) of the dislocation *J* located at $x_1 = x_1^{'} \equiv vt$ in the medium may be deduced from those (moving sinusoidal dislocations) located at $x_1 = x_1^{'}$ with simple form $A_n = \xi_n \sin \kappa_n x_3$ in x_2x_3-planes ***(Figure 2)***. For the later, the elastic fields at $\vec{x} = (x_1, x_2, x_3)$ are (to linear term in amplitude ξ_n)

$$\vec{u}^{(J)(n)}(\vec{x}) = \vec{u}^{(J)(0)}(y_1, x_2) + \vec{u}^{(J)A_n}(y_1, x_2, x_3),$$
$$(\sigma)^{(J)(n)}(\vec{x}) = (\sigma)^{(J)(0)}(y_1, x_2) + (\sigma)^{(J)A_n}(y_1, x_2, x_3) \quad (2)$$

$y_1 = x_1 - x_1^{'}$; $\vec{u}^{(J)(0)}$ and $(\sigma)^{(J)(0)}$ are of zero order, they correspond to the fields of a moving straight dislocation *J* (parallel to x_3) at $x_1 = x_1^{'}$ on Ox_1x_3 with Burgers vector $\vec{b}_J$; $\vec{u}^{(J)A_n}$ and $(\sigma)^{(J)A_n}$ are oscillating parts involving A_n or its spatial x_3 -derivative $\partial A_n / \partial x_3$.

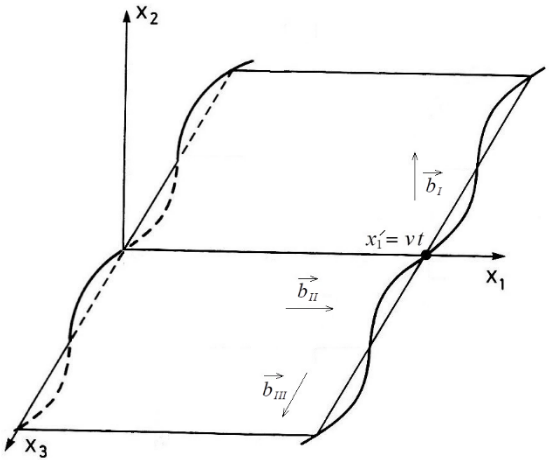

Figure 2 : *Infinitely long sinusoidal dislocation travelling uniformly at constant speed v in the x_1- direction with Burgers vector $\vec{b}_J$ directed along x_1(J=II), x_2 (J=I) and x_3 (J= III); the dislocation at the origin (t=0) and after incremental time t are illustrated*

When the dislocation exhibits shape *f* (1), the elastic fields take the form

$$\vec{u}^{(J)}(\vec{x}) = \vec{u}^{(J)(0)}(y_1, y_2) + \sum_n \vec{u}^{(J)A_n}(y_1, y_2, x_3) \equiv \vec{u}^{(J)(0)} + \vec{u}^{(J)\xi},$$
$$(\sigma)^{(J)}(\vec{x}) = (\sigma)^{(J)(0)}(y_1, y_2) + \sum_n (\sigma)^{(J)A_n}(y_1, y_2, x_3) \equiv (\sigma)^{(J)(0)} + (\sigma)^{(J)\xi} \qquad (3)$$

$y_2 = x_2 - h$; here A_n stands for $A_n = \xi_n \sin\kappa_n x_3 + \delta_n \cos\kappa_n x_3$. In Section 2 (Methodology), the procedure for determining the dislocation *J* elastic fields and crack analysis are presented. In Section 3 are listed expressions of the dislocation elastic fields, distribution functions of crack dislocations, crack-tip stresses and crack extension force. A numerical application is given with a special non-planar crack in Section 4. Sections 5 and 6 are devoted to the discussion and conclusion, respectively.

II - METHODOLOGY

II-1. Elastic fields of uniformly moving crack dislocations

The three types *J (J=I, II* and *III)* of crack dislocation considered have Burgers vectors $\vec{b}_I = (0, b, 0)$, $\vec{b}_{II} = (b, 0, 0)$ and $\vec{b}_{III} = (0, 0, b)$; they spread in the x_2x_3-plane located at $x_1 = x_1' \equiv vt$ in the form of a Fourier series *f* (1). We shall make use of the displacement $u_m(\vec{x},t)$, m=1, 2 and 3, (see (5) below) due to a plastic distortion $\beta^*_{ij}(\vec{x},t)$ given as a periodic function of coordinates and time

$$\beta^*_{ij} = \bar{\beta}^*_{ij}(\vec{k},\omega)e^{i(\omega t+\vec{k}.\vec{x})} \tag{4}$$

where $\vec{k}=(k_1,k_2,k_3)$ and ω are arbitrary constants. Mura [8, 9] has shown the associated displacement component to be

$$u_m(\vec{x},t) = -ik_l C_{klji} L_{mk} \bar{\beta}^*_{ij} e^{i(\omega t+\vec{k}.\vec{x})} \tag{5}$$

For isotropic material,

$$L_{mk}(\vec{k},\omega) = \frac{\delta_{km}\left((\lambda+2\mu)k^2-\rho\omega^2\right)-k_k k_m(\lambda+\mu)}{\left(\mu k^2-\rho\omega^2\right)\left((\lambda+2\mu)k^2-\rho\omega^2\right)} \tag{6}$$

where $k^2 = k_1^2+k_2^2+k_3^2$ and

$$C_{klji} = \lambda\delta_{kl}\delta_{ji}+\mu\delta_{kj}\delta_{li}+\mu\delta_{ki}\delta_{lj}\,, \tag{7}$$

δ_{ij} being the Kronecker delta and λ and μ are Lamé's constants. The plastic distortions $\beta^{*(J)}_{ij}(\vec{x},t)$ associated to the dislocations J (J= I , II and III), are expressed successively to first order in ξ, assuming ξ in (1) small.

$$\beta^{*(I)}_{12}(\vec{x},t) = b\delta(y_1)H(y_2) - b\xi\delta(y_1)\delta(y_2) \tag{8}$$

the other components of the plastic distortion are zero; δ and H are the Dirac delta and Heaviside step functions, respectively; $y_1 = x_1 - vt$ and $y_2 = x_2 - h$. Here, the first term is due to a straight edge dislocation displaced by $x_2 = h$ from the Ox_1x_3- plane. The corresponding displacement can be derived by replacing x_2 by $(x_2 - h)$ in the displacement of a straight edge I dislocation at $x_1 = x_1' \equiv vt$ (travelling in the Ox_1x_3- plane at velocity v in the x_1- direction; in the present geometry, see [10]). We shall therefore concentrate on the second term denoted $\beta^{*(I)\xi}_{12}$. Its Fourier form is taken from [5]:

$$\beta^{*(I)\xi}_{12} = -\frac{b}{8\pi^2}\sum_n \int_{-\infty}^{\infty}\int_{-\infty}^{\infty}\left(z_n e^{i(\omega t+\vec{k}'.\vec{x}_h)} + \bar{z}_n e^{i(\omega t+\vec{k}.\vec{x}_h)}\right)dk_1 dk_2 \tag{9}$$

$\vec{k}^{'}=(k_1^{'}=k_1,k_2^{'}=k_2,k_3^{'}=-\kappa_n)$, $\vec{k}=(k_1,k_2,k_3=\kappa_n)$, $\vec{x}_h=(x_1,y_2,x_3)$;
$z_n=\delta_n+i\xi_n$, $\bar{z}_n=\delta_n-i\xi_n$, $\omega=-k_1 v$.

$\beta_{12}^{*(I)\xi}$(9) is a superposition of wave expressions of the form (4). Therefore, associated displacement $u_m^{(I)\xi}(\vec{x},t)$ is a similar superposition of the displacement (5) :

$$u_m^{(I)\xi}=-\frac{b}{8\pi^2}\sum_n\int_{-\infty}^{\infty}\int_{-\infty}^{\infty}\Big(-ik_l^{'}C_{kl21}L_{mk}(\vec{k}^{'},\omega)z_n e^{i(\omega t+\vec{k}^{'}.\vec{x}_h)} -ik_l C_{kl21}L_{mk}(\vec{k},\omega)\bar{z}_n e^{i(\omega t+\vec{k}.\vec{x}_h)}\Big)dk_1dk_2 \tag{10}$$

We now consider the dislocation *J= II* with form (1) at $x_1=x_1^{'}\equiv vt$. For convenience, we follow the presentation in [5]. The elastic fields due to this dislocation can be derived from those of a sinusoidal dislocation located at $x_1=x_1^{'}$ with the same Burgers vector, lying in the x_2x_3- plane and defined by $x_2=A_n\equiv\xi_n\sin\kappa_n x_3$ (see ***Figure 2*** for illustration). There are two non-zero components of the plastic distortion:

$$\beta_{21}^{*(II)(n)}=\frac{b}{1+(\partial A_n/\partial x_3)^2}\delta(x_2-A_n)H(-y_1),$$
$$\beta_{31}^{*(II)(n)}=-\partial A_n/\partial x_3\beta_{21}^{*(II)(n)} \tag{11}$$

We assume that both A_n and $\partial A_n/\partial x_3$ are small in magnitude: corresponding Fourier forms used in the sequel are

$$\beta_{21}^{*(II)(n)}=\beta_{21}^{*(II)(0)}+\beta_{21}^{*(II)A_n}$$
$$\beta_{21}^{*(II)(0)}=\frac{ib}{(2\pi)^2}\int_{-\infty}^{\infty}\int_{-\infty}^{\infty}\frac{1}{k_1}e^{i(\omega t+k_1x_1+k_2x_2)}dk_1dk_2,$$
$$\beta_{21}^{*(II)A_n}=\frac{ib\xi_n}{8\pi^2}\int_{-\infty}^{\infty}\int_{-\infty}^{\infty}\frac{k_2}{k_1}\Big(e^{i(\omega t+\vec{k}^{'}.\vec{x})}-e^{i(\omega t+\vec{k}.\vec{x})}\Big)dk_1dk_2 \tag{12}$$
$$\beta_{31}^{*(II)(n)}=-\frac{ib\kappa_n\xi_n}{8\pi^2}\int_{-\infty}^{\infty}\int_{-\infty}^{\infty}\frac{1}{k_1}\Big(e^{i(\omega t+\vec{k}^{'}.\vec{x})}+e^{i(\omega t+\vec{k}.\vec{x})}\Big)dk_1dk_2 \tag{13}$$

$\beta_{21}^{*(II)(0)}$ corresponds to a straight edge dislocation located at $x_1=x_1^{'}$ in Ox_1x_3;

the corresponding elastic fields in the present study are known [10]. In these fields, we just replace x_2 by (x_2-h) to obtain the elastic fields of the straight dislocation at $x_1 = x_1^{'}$ displaced by $x_2 = h$ from the Ox_1x_3-plane. This gives the non-oscillating part of the elastic fields of crack dislocations *II* with form *f* (1). With two non-zero components $\beta_{21}^{*(II)}$ and $\beta_{31}^{*(II)}$, their oscillating parts for the displacement read :

$$u_m^{(II)\xi} = -i\mu \sum_n \int_{-\infty}^{\infty}\int_{-\infty}^{\infty} \Big(\Big[(k_1 L_{m2}^{'} + k_2 L_{m1}^{'}) \overline{\beta}_{21}^{*(II)A_n}(\vec{k}^{'},\omega)$$
$$+ (k_1 L_{m3}^{'} - \kappa_n L_{m1}^{'}) \overline{\beta}_{31}^{*(II)(n)}(\vec{k}^{'},\omega) \Big] e^{i(\omega t + \vec{k}^{'}.\vec{x}_h)} + \Big[(k_1 L_{m2} + k_2 L_{m1}) \overline{\beta}_{21}^{*(II)A_n}(\vec{k}\ ,\omega)$$
$$+ (k_1 L_{m3} + \kappa_n L_{m1}) \overline{\beta}_{31}^{*(II)(n)}(\vec{k}\ ,\omega) \Big] e^{i(\omega t + \vec{k}.\vec{x}_h)} \Big) dk_1 dk_2 \qquad (14)$$

$$\overline{\beta}_{21}^{*(II)A_n}(\vec{k}^{'},\omega) = -\overline{\beta}_{21}^{*(II)A_n}(\vec{k}\ ,\omega) = \frac{ib\xi_n k_2}{8\pi^2 k_1},$$

$$\overline{\beta}_{31}^{*(II)(n)}(\vec{k}^{'},\omega) = \overline{\beta}_{31}^{*(II)(n)}(\vec{k}\ ,\omega) = -\frac{ib\kappa_n \xi_n}{8\pi^2 k_1} \qquad (15)$$

$$L_{mk}^{'} = L_{mk}(\vec{k}^{'},\omega), \quad L_{mk} = L_{mk}(\vec{k},\omega).$$

For the average screw dislocation *III* with form *f* (1) at $x_1 = x_1^{'}$, the non-zero component of the plastic distortion used previously [5] is written to first order in ξ :

$$\beta_{13}^{*(III)}(\vec{x},t) = b\delta(y_1)H(y_2) - b\xi\delta(y_1)\delta(y_2) \qquad (16)$$

Here, the first term $\beta_{13}^{*(III)(0)}$ is due to a straight screw at $x_1 = x_1^{'}$ with elevation $x_2 = h$ from Ox_1x_3. Its Fourier form reads

$$\beta_{13}^{*(III)(0)} = \int_{-\infty}^{\infty}\int_{-\infty}^{\infty} \overline{\beta}_{13}^{*(III)(0)} e^{i(\omega t + k_1 x_1 + k_2 y_2)} dk_1 dk_2 \qquad (17)$$
$$\overline{\beta}_{13}^{*(III)(0)} = -\frac{ib}{4\pi^2 k_2}.$$

Using the displacement (5) associated with a single wave plastic distortion, we obtain

$$u_m^{(III)(0)} = \int_{-\infty}^{\infty}\int_{-\infty}^{\infty} -ik_l\, C_{kl31} L_{mk} \bar{\beta}_{13}^{*(III)(0)} e^{i\left(\omega t + k_1 x_1 + k_2 (x_2 - h)\right)} dk_1 dk_2 \tag{18}$$

Because $\beta_{13}^{*(III)}$ (16) and $\beta_{12}^{*(I)}$ (8) are identical in form, we can make use of the Fourier form (9) for the second term $\beta_{13}^{*(III)\xi}$ in (16). Using (5), we obtain the associated displacement $u_m^{(III)\xi}(\vec{x},t)$ to be

$$u_m^{(III)\xi} = \sum_n \int_{-\infty}^{\infty}\int_{-\infty}^{\infty} \bar{\beta}_{13}^{*(III)A_n} \Big(-ik_l^{'} C_{kl31} L_{mk}^{'} e^{i(\omega t + \vec{k}'.\vec{x}_h)} + ik_l C_{kl31} L_{mk}(\vec{k},\omega) e^{i(\omega t + \vec{k}.\vec{x}_h)} \Big) dk_1 dk_2 \tag{19}$$

$$\bar{\beta}_{13}^{*(III)A_n} = -\frac{ib\xi_n}{8\pi^2}.$$

At this stage, we can write down the various displacements $\vec{u}^{(J)}$ ($J = I$, II and III) associated with the three types J of crack dislocation with form f (1). The stress fields $(\sigma)^{(J)}$ can be obtained by differentiating the displacements. Our calculation results are displayed in Section 3.

II-2. Crack analysis

The crack system ***(Figure 1)*** has been described earlier in Section 1. The requirements are that *(i)* the front (x_2x_3- plane) of the crack moves at constant velocity v along the x_1- direction and *(ii)* the crack faces remain free from any traction. The latter condition reads

$$\begin{cases} \bar{\sigma}_{12} - \partial f/\partial x_1 \bar{\sigma}_{11} - \partial f/\partial x_3 \bar{\sigma}_{13} = 0 \\ \bar{\sigma}_{22} - \partial f/\partial x_1 \bar{\sigma}_{12} - \partial f/\partial x_3 \bar{\sigma}_{23} = 0 \\ \bar{\sigma}_{23} - \partial f/\partial x_1 \bar{\sigma}_{13} - \partial f/\partial x_3 \bar{\sigma}_{33} = 0 \end{cases} \tag{20}$$

$\bar{\sigma}_{ij}$ stands for the total stress at any point $P(x_1, x_2, x_3)$ in the medium and is linked to D_J. In (20), we are concerned with the positions on the crack faces only. We write $\bar{\sigma}_{ij}$ as

$$\bar{\sigma}_{ij} = \sigma_{ij}^{A} + \sigma_{ij}^{(C)(I)} + \sigma_{ij}^{(C)(II)} + \sigma_{ij}^{(C)(III)} \tag{21}$$

$(\sigma)^A$ is the externally applied stress including normal induced stresses from Poisson effect,

$$(\sigma)^A = \begin{pmatrix} -\nu_A \sigma_{22}^a & \sigma_{12}^a & 0 \\ \sigma_{12}^a & \sigma_{22}^a & \sigma_{23}^a \\ 0 & \sigma_{23}^a & -\nu_A \sigma_{22}^a \end{pmatrix} \tag{22}$$

$$\sigma_{ij}^{(C)(J)}(x_1, x_2, x_3) = \int_{-c}^{c} \sigma_{ij}^{(J)}(x_1 - x_1', x_2, x_3) D_J(x_1') dx_1' \quad (J = I,\ II \text{ and } III) \tag{23}$$

$\sigma_{ij}^{(J)}$ is the stress due to the crack dislocation J located at $x_1 = x_1'$ in the distribution. (20) gives three integral equations the resolution of which yields the D_J. The relative displacements ϕ_J of the faces of the crack in the x_1-direction (J=*II*), x_2- direction (J=*I*) and x_3- direction (J=*III*) are obtained by integration from the relation $d\phi_J = -bD_J(x_1')dx_1'$:

$$\phi_J(x_1) = \int_{x_1}^{c} bD_J(x_1')dx_1' ,\ |x_1| \le c \tag{24}$$

From (21) to (23), one can obtain the crack-tip stresses. The crack extension force G per unit length of the crack front is defined in previous works (see [5, 6, 10, 11], for example). ***Figure 3*** is a schematic representation of simple special cracks captured by the modelling. The cracks extend in the $x_1 -$direction from $x_1 = -c$ to c and must be considered to run indefinitely in the $x_3 -$direction. The crack shape in planes perpendicular to x_1 is described by ξ (***Figure 3c*** for example). The shape f of the crack in planes perpendicular to x_3 is given by both ξ, through the $x_1 -$dependence of positive quantities ξ_n, δ_n and κ_n (1), and function $h = h(x_1)$. Since ξ is assumed to be small oscillating function, the average fracture plane is described correctly by the equation $x_2 = h(x_1)$. When $\xi = 0$, the crack dislocations are straight parallel to x_3 and distributed over the surface $x_2 = h(x_1)$. Specific examples are ***(Figure 3)*** :

- $h(x_1) = p_0 x_1$ ($p_0 \ge 0$) and $\xi = 0$. This corresponds to a planar crack π_0 (with a straight front parallel to x_3) rotated around Ox_3 by angle $\theta_0 = \tan^{-1} p_0$ from Ox_1x_3, ***Figure 3a***.
- $h(x_1)$ is an arbitrary function of x_1, $\xi = 0$. The sketch in ***Figure 3b*** corresponds to h odd although this is not mandatory. Actually h odd conforms well to homogeneity of the medium, geometry of the applied loadings and D_J (Section 3) approximations adopted in the present study.

- $h(x_1) = p_0 x_1$ ($p_0 \geq 0$) and $\xi = \xi(x_3)$ independent of x_1. The crack fluctuates about plane π_0 with a front spreading in planes parallel to $x_2 x_3$ in the form ξ. In the example displayed in ***Figure 3c*** the crack consists of planar facets with inclination angles ϕ_A and ϕ_B ***(Figure 3d)*** at points *A* and *B* of the crack front located on the average fracture plane.

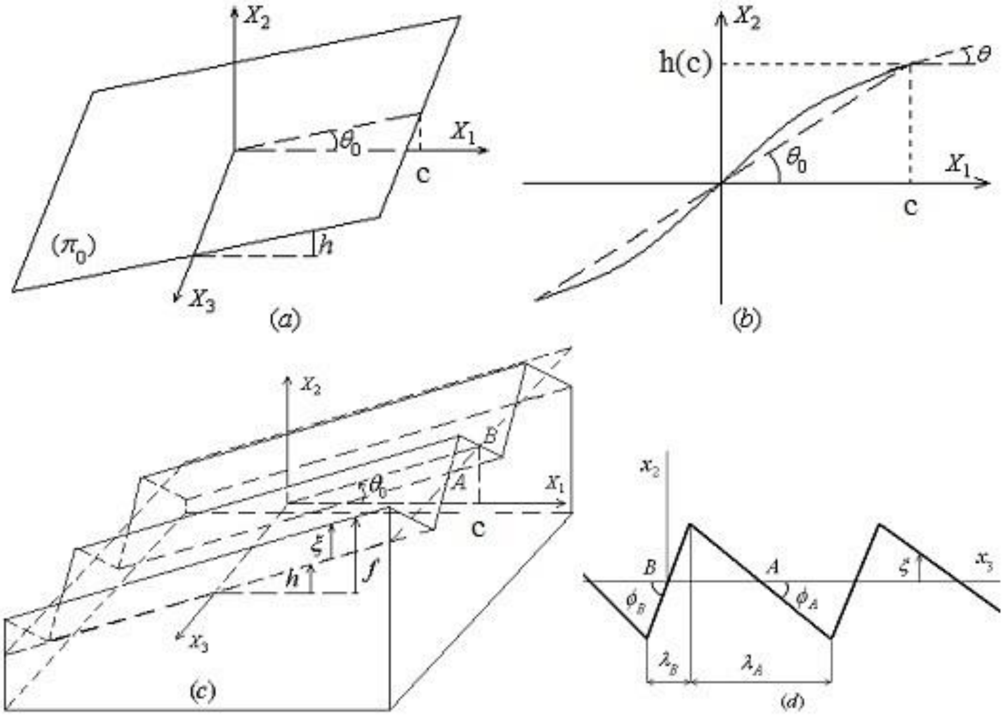

Figure 3 : *Simple special cracks. (a) Inclined planar crack π_0 (see text). (b) A non-planar crack (parallel to x_3) as h odd function of x_1 ($x_2 = h(x_1)$). (c) Non-planar crack fluctuating about an average inclined plane π_0. The crack consists of planar facets; its fronts at $x_1 = \pm c$ lie in $x_2 x_3 -$ planes. At $x_1 = c$, the crack front is characterized by inclination angles ϕ_A and ϕ_B (see (d)) at points A and B located on the average fracture plane. (d) Sketch of the crack front in (c) with B taken as origin. In this geometry (from (a) to (c)) the general loading of the crack systems corresponds to uniform applied σ_{22}^a, σ_{12}^a and σ_{23}^a at infinity in the x_2, x_1 and x_3 directions, respectively*

III - RESULTS

III-1. Elastic fields of crack dislocation *I*

We consider a dislocation *I* with Burgers vector $\vec{b}_I = (0, b, 0)$ lying indefinitely in the x_3- direction and spreading in the x_2x_3- plane at $x_1 = x_1^{'} \equiv vt$ in the Fourier series form *f* (1). The elastic fields take form (3). We get at spatial position (x_1, x_2, x_3) :

$$u_m^{(I)(0)} = \frac{b}{\pi \tilde{v}_t^2}\left(\delta_{m1}\left[\frac{1}{P_l}\ln r_l - \frac{P_{2t}^2}{P_t}\ln r_t\right] + \delta_{m2}\left[\tan^{-1}\frac{y_1}{P_l y_2} - \frac{P_{2t}^2}{P_t^2}\tan^{-1}\frac{y_1}{P_t y_2}\right]\right) \qquad (25)$$

$$\sigma_{11}^{(I)(0)} = \frac{\mu b}{\pi \tilde{v}_t^2} y_1 \left(\frac{2+(1-2c_*^2)\tilde{v}_t^2}{P_l r_l^2} - \frac{2P_{2t}^2}{P_t r_t^2}\right),$$

$$\sigma_{22}^{(I)(0)} = \frac{2\mu b P_{2t}^2}{\pi \tilde{v}_t^2} y_1 \left(\frac{1}{P_t r_t^2} - \frac{1}{P_l r_l^2}\right),$$

$$\sigma_{33}^{(I)(0)} = \frac{\mu b (1-2c_*^2)}{\pi P_l}\frac{y_1}{r_l^2},$$

$$\sigma_{21}^{(I)(0)} = \frac{2\mu b}{\pi \tilde{v}_t^2} y_2 \left(\frac{P_l}{r_l^2} - \frac{P_{2t}^4}{P_t r_t^2}\right) \qquad (26)$$

$$\tilde{v}_t = v / c_t,\; P_t^2 = 1-\tilde{v}_t^2,\; P_{2t}^2 = 1-\tilde{v}_t^2/2;$$
$$\tilde{v}_l = v / c_l,\; P_l^2 = 1-\tilde{v}_l^2; \quad r_s^2 = y_1^2 + P_s^2 y_2^2, \quad s=t \text{ and } l; \quad c_* = c_t / c_l;$$

the subscript *m* takes the values 1 and 2, and c_t and c_l are the velocities of transverse and longitudinal sound waves, respectively. Other elastic field components are zero. The oscillating parts of the elastic fields take the forms:

$$u_1^{(I)\xi} = \frac{b}{\pi \tilde{v}_t^2}\sum_n A_n \frac{\partial}{\partial x_2}\left(-\frac{P_{2t}^2}{P_t}K_0[z_n^{(t)}] + \frac{2(1-\nu)c_*^2}{(1-2\nu)P_l}K_0[z_n^{(l)}]\right),$$

$$u_2^{(I)\xi} = \frac{b}{2\pi \tilde{v}_t^2}\sum_n A_n \left(\frac{\tilde{v}_t^2}{P_t}\frac{\partial}{\partial y_1}K_0[z_n^{(t)}] + 2\frac{\partial^2}{\partial x_2^2}\left[\frac{1}{P_t}\bar{I}^{(t)} - \frac{2(1-\nu)c_*^2}{(1-2\nu)P_l}\bar{I}^{(l)}\right]\right),$$

$$u_3^{(I)\xi} = \frac{b(1-c_*^2)}{\pi \tilde{v}_t^2}\sum_n \frac{\partial A_n}{\partial x_3}\frac{\partial}{\partial x_2}\left(\frac{(1-2\nu)c_*^{-2}}{P_t}\bar{I}^{(t)} - \frac{2(1-\nu)}{P_l}\bar{I}^{(l)}\right) \qquad (27)$$

$$\sigma_{ii}^{(I)\xi} = \frac{2\mu}{1-2\nu}\left(\left[\delta_{i1}(1-\nu)+\nu(\delta_{i2}+\delta_{i3})\right]\frac{\partial u_1^{(I)\xi}}{\partial x_1} + \left[\delta_{i2}(1-\nu)+\nu(\delta_{i1}+\delta_{i3})\right]\frac{\partial u_2^{(I)\xi}}{\partial x_2} \right.$$

$$\left. + \left[\delta_{i3}(1-\nu)+\nu(\delta_{i1}+\delta_{i2})\right]\frac{\partial u_3^{(I)\xi}}{\partial x_3} \right), \ i\text{=1, 2 and 3,}$$

$$\sigma_{ij}^{(I)\xi} = \mu\left(\frac{\partial u_i^{(I)\xi}}{\partial x_j} + \frac{\partial u_j^{(I)\xi}}{\partial x_i} \right), \quad i \neq j \tag{28}$$

$$z_n^{(s)} = (\kappa_n / P_s)\sqrt{y_1^2 + P_s^2 y_2^2}\,, \quad \overline{I}^{(s)} = \int_{y_1}^{\infty} K_0[z_n^{'(s)}]\, dy\,,\ s = t \text{ and } l;$$

$K_n[z]$ is the nth- order modified Bessel function usually so denoted and $z_n^{'(s)}$ stands for $z_n^{(s)}$ with y instead of y_1.

III-2. Elastic fields of crack dislocation *II*

The dislocation *II* has Burgers vector $\vec{b}_{II} = (b, 0, 0)$ and spreads in the x_2x_3-plane at $x_1 = x_1^{'} \equiv vt$ in the Fourier series form f (1). The elastic fields have form (3). We obtain:

$$u_m^{(II)(0)} = \frac{b}{\pi \tilde{v}_t^2}\left(\delta_{m2}\left[P_l \ln r_l - \frac{P_{2t}^2}{P_t}\ln r_t \right] + \delta_{m1}\left[P_{2t}^2 \tan^{-1}\frac{y_1}{P_t y_2} - \tan^{-1}\frac{y_1}{P_l y_2} \right] \right) \tag{29}$$

$$\sigma_{11}^{(II)(0)} = \frac{\mu b}{\pi \tilde{v}_t^2} y_2 \left(\frac{2P_t P_{2t}^2}{r_t^2} + \frac{P_l[(c_*^{-2}-2)P_l^2 - c_*^{-2}]}{r_l^2} \right),$$

$$\sigma_{22}^{(II)(0)} = \frac{\mu b}{\pi \tilde{v}_t^2} y_2 \left(\frac{P_l[P_l^2 c_*^{-2} - c_*^{-2} + 2]}{r_l^2} - \frac{2P_t P_{2t}^2}{r_t^2} \right),$$

$$\sigma_{33}^{(II)(0)} = -\frac{\mu b(1-2c_*^2)P_l}{\pi}\frac{y_2}{r_l^2},$$

$$\sigma_{21}^{(II)(0)} = \frac{2\mu b}{\pi \tilde{v}_t^2} y_1 \left(\frac{P_l}{r_l^2} - \frac{P_{2t}^4}{P_t r_t^2} \right) \tag{30}$$

Other elastic fields of zero order with respect to A_n are zero. The oscillating parts of the displacement are :

$$
\begin{aligned}
u_1^{(II)\xi} = \frac{b}{2\pi\tilde{v}_t^2}\sum_n A_n \Bigg(\frac{\partial}{\partial y_1}\left[\frac{4(1-\nu)c_*^2 P_l}{1-2\nu} K_0[z_n^{(l)}] - (2-\tilde{v}_t^2) P_t K_0[z_n^{(t)}] \right] \\
- \frac{\kappa_n^2 \tilde{v}_t^2 \left[(1-2\nu)c_*^{-2} - 2(1-\nu) \right] \bar{I}^{(t)}}{P_t} + \pi\delta(y_2)\,\mathrm{sgn}\, y_1 \Bigg[\tilde{v}_t^2 - 2 + \frac{4(1-\nu)c_*^2}{1-2\nu} \\
- y_1^2 \frac{\kappa_n^2 \left[(1-2\nu)c_*^{-2} - 2(1-\nu) \right]}{2} \Bigg] \Bigg),
\end{aligned}
$$

$$
\begin{aligned}
u_2^{(II)\xi} = \frac{b}{2\pi\tilde{v}_t^2}\sum_n A_n \frac{\partial}{\partial y_2} \Bigg(\left[\frac{2(1-\nu)c_*^2}{1-2\nu} - 1 \right] 2\pi\delta(y_2)|y_1| - \frac{(2-\tilde{v}_t^2) K_0[z_n^{(t)}]}{P_t} \\
+ \frac{4(1-\nu)c_*^2 P_l}{1-2\nu} K_0[z_n^{(l)}] \Bigg),
\end{aligned}
$$

$$
\begin{aligned}
u_3^{(II)\xi} = \frac{b}{2\pi\tilde{v}_t^2}\sum_n \frac{\partial A_n}{\partial x_3} \Bigg(4(1-\nu)(1-c_*^2) P_l K_0[z_n^{(l)}] + \frac{(1-2\nu)(1-c_*^{-2})(2-\tilde{v}_t^2) K_0[z_n^{(t)}]}{P_t} \\
+ \left[(1-2\nu)(2-c_*^{-2}) - 2(1-\nu)(2c_*^2 - 1) \right] \pi\delta(y_2)|y_1| \Bigg) \qquad (31)
\end{aligned}
$$

The associated stress fields are obtained by differentiating the displacements with similar relations as in (28).

III-3. Elastic fields of crack dislocation *III*

The dislocation *III* has Burgers vector $\vec{b}_{III} = (0,0,b)$ and spreads in the x_2x_3-plane at $x_1 = x_1' \equiv vt$ in the Fourier series form *f* (1). The elastic fields have form (3). For the non-oscillating part of the displacement, the only non-zero component is

$$
u_3^{(III)(0)} = \frac{b}{2\pi\beta_{13(t)}^2} \tan^{-1}\frac{P_t y_2}{y_1} \qquad (32)
$$

$\beta_{13(t)}^2$ stands for P_t^2. Surprisingly $\beta_{13(t)}^2 = 1$ when the displacement $u_3^{(III)(0)}$ is derived from the plastic distortion $\beta_{23}^*(\vec{x},t)$ for which it is assumed that a slip *b* = (0,0,*b*) is produced in the x_1x_3- plane for $x_1 < vt$ [8, 12]. Hence, it is questioned to see the effect of this difference in both values of $u_3^{(III)(0)}$. We observe no change in the reduced crack extension force (see ***Figure 6*** in Section 4) for a special non-planar crack with a segmented front.

$$\sigma_{13}^{(III)(0)} = -\frac{\mu b P_t}{2\pi\beta_{13(t)}^2}\frac{y_2}{r_t^2}, \quad \sigma_{23}^{(III)(0)} = \frac{\mu b P_t}{2\pi\beta_{13(t)}^2}\frac{y_1}{r_t^2} \tag{33}$$

The compressive $\sigma_{ii}^{(III)(0)}$ (i=1, 2 and 3) stresses are zero, as also $\sigma_{21}^{(III)(0)}$. The oscillating parts of the displacement read:

$$u_1^{(III)\xi} = \frac{b}{2\pi\tilde{v}_t^2}\sum_n \frac{\partial A_n}{\partial x_3}\left(\frac{\tilde{v}_t^2 - 2(c_*^{-2}-1)(1-2\nu)}{P_t}K_0[z_n^{(t)}] + \frac{4(1-\nu)(1-c_*^2)}{P_l}K_0[z_n^{(l)}]\right),$$

$$u_2^{(III)\xi} = \frac{b(c_*^{-2}-1)}{\pi\tilde{v}_t^2}\sum_n \frac{\partial A_n}{\partial x_3}\frac{\partial}{\partial x_2}\left(\frac{1-2\nu}{P_t}\bar{I}^{(t)} - \frac{2(1-\nu)c_*^2}{P_l}\bar{I}^{(l)}\right) \tag{34}$$

$$u_3^{(III)\xi} = \frac{b}{2\pi\tilde{v}_t^2}\sum_n A_n\left(\frac{\tilde{v}_t^2}{P_t}\frac{\partial K_0[z_n^{(t)}]}{\partial y_1} - 2\kappa_n^2(c_*^{-2}-1)\left[\frac{(1-2\nu)\bar{I}^{(t)}}{P_t} - \frac{2(1-\nu)c_*^2}{P_l}\bar{I}^{(l)}\right]\right).$$

The associated stress fields $(\sigma)^{(J)\xi}$ are obtained by differentiating the displacements.

III-4. Crack dislocation distributions

Assume first that the dislocations are straight parallel to the x_3-direction $(\xi = 0)$ and $h(x_1) = p_0 x_1$ depends linearly on x_1 with p_0 positive constant ***(Figure 3a)***. We thus have a planar crack of finite extension, with straight fronts running indefinitely along x_3, rotated (from Ox_1x_3) about the positive x_3-direction by $\theta_0 = \tan^{-1} p_0$. The crack extends from $x_1 = -c$ to c and is subjected to mixed mode I+II+III with loadings applied at infinity. Under such conditions, we have $\partial f/\partial x_1 = \partial h/\partial x_1 = p_0$, $\partial f/\partial x_3 = \partial\xi/\partial x_3 = 0$; making use of the traction -free crack face condition (20) and stresses from moving straight dislocations J, the dislocation distributions D_J are obtained in the form

$$D_J(x_1) = d_J D_0^{(J)}(x_1), \qquad J = I, II \text{ and } III \tag{35}$$

$D_0^{(J)}$ corresponds to the equilibrium distribution of straight dislocations J when the crack is planar in the Ox_1x_3- plane (p_0= 0), extending from x_1= -c to c, under pure mode J loading (see [10] for J=I and II). The calculation results are listed ($M_{12} = \sigma_{21}^a/\sigma_{22}^a$) :

$$D_0^{(I)}(x_1) = \frac{\sigma_{22}^a}{\pi C_0^{(I)}} \frac{x_1}{\sqrt{c^2 - x_1^2}}, \qquad C_0^{(I)} = \frac{\mu b\left(2 - \tilde{v}_t^2\right)}{\pi \tilde{v}_t^2}\left(\frac{1}{P_t} - \frac{1}{P_l}\right),$$

$$d_I = \frac{(M_{12} + \nu_A p_0)(C^{(II)(1)} / C^{(II)(2)}) - 1 + p_0 M_{12}}{C^{(I)} / C_0^{(I)}},$$

$$C^{(II)(1)} = \frac{\mu b p_0}{\pi}\left(\frac{P_{2t}^2}{P_t\left(1 + p_0^2 P_t^2\right)} - \frac{P_l}{1 + p_0^2 P_l^2}\right),$$

$$C^{(II)(2)} = \frac{\mu b}{\pi \tilde{v}_t^2}\left(\frac{P_l\left[2 + p_0^2\left\{2 + (1 - 2c_*^2)\tilde{v}_t^2\right\}\right]}{1 + p_0^2 P_l^2} - \frac{2P_{2t}^2(P_{2t}^2 + p_0^2 P_t^2)}{P_t(1 + p_0^2 P_t^2)}\right),$$

$$C^{(I)} = \frac{C^{(I)(2)} C^{(II)(1)} - C^{(II)(2)} C^{(I)(1)}}{C^{(II)(2)}},$$

$$C^{(I)(1)} = \frac{2\mu b}{\pi \tilde{v}_t^2}\left(\frac{P_{2t}^2\left(1 + p_0^2 P_{2t}^2\right)}{P_t\left(1 + p_0^2 P_t^2\right)} - \frac{P_{2t}^2 + p_0^2 P_l^2}{P_l\left(1 + p_0^2 P_l^2\right)}\right),$$

$$C^{(I)(2)} = \frac{\mu b p_0}{\pi}\left(\frac{P_{2t}^2}{P_t\left(1 + p_0^2 P_t^2\right)} - \frac{1}{P_l\left(1 + p_0^2 P_l^2\right)}\right);$$

$$D_0^{(II)}(x_1) = \frac{\sigma_{21}^a}{\pi C_0^{(II)}} \frac{x_1}{\sqrt{c^2 - x_1^2}}, \qquad C_0^{(II)} = \frac{2\mu b\left(P_t P_l - P_{2t}^4\right)}{\pi \tilde{v}_t^2 P_t},$$

$$d_{II} = \frac{(1 - p_0 M_{12})(C^{(I)(2)} / C^{(I)(1)}) - M_{12} - \nu_A p_0}{M_{12}(C^{(II)} / C_0^{(II)})}, \qquad C^{(II)} = C^{(I)} \frac{C^{(II)(2)}}{C^{(I)(1)}};$$

$$D_0^{(III)}(x_1) = \frac{\sigma_{23}^a}{\pi C_0^{(III)}} \frac{x_1}{\sqrt{c^2 - x_1^2}}, \qquad C_0^{(III)} = \frac{\mu b P_t}{2\pi \beta_{13(t)}^2}, \qquad d_{III} = \frac{1 + p_0^2 P_t^2}{1 + p_0^2} \tag{36}$$

The corresponding relative displacements ϕ_J of the faces of the crack, in the x_2 ($J=I$), x_1 ($J = II$) and x_3 ($J = III$) directions, are

$$\phi_J(x_1) = d_J \phi_0^{(J)}(x_1) \tag{37}$$

$\phi_0^{(J)}$ corresponds to the relative displacement of the crack faces when the crack is in Ox_1x_3- plane under pure mode J loading. They are given by [10] for $J=I$ and II. We have

$$\phi_0^{(J)}(x_1) = \frac{b}{\pi}\left(\frac{\sigma_{22}^a}{C_0^{(I)}}\delta_{JI} + \frac{\sigma_{21}^a}{C_0^{(II)}}\delta_{JII} + \frac{\sigma_{23}^a}{C_0^{(III)}}\delta_{JIII}\right)\sqrt{c^2 - x_1^2}\,, \quad J = I, II \text{ and } III \tag{38}$$

D_J is unbounded at $x_1 = \pm c$ and the corresponding ϕ_J vertical at these end points. In its general form (20) requires a numerical resolution. We shall progress further by providing approximate expressions for the stress about the crack front and crack extension force with f given by (1) using D_J (35) when the average fracture surface $h=h(x_1)$ can be approximated by plane π_0 of ***Figure 3a***.

III-5. Stresses about the crack-tip

We consider $P\ (x_1, x_2, x_3)$ about the crack front located at $x_1 = c$; hence x_2 is close to h since the fracture surface is given by $f = h + \xi$ with ξ small. Writing $x_1 = c + s$ $(0 < s << c)$, from (21) the stress at P is identified to the following formula:

$$\sigma_{ij}^{(C)}(s, x_2, x_3) = \sum_{J=I}^{III} \int_{c-\delta c}^{c} \sigma_{ij}^{(J)}(c + s - x_1', x_2, x_3) D_J(x_1') dx_1', \qquad \delta c << c \tag{39}$$

This stress expression means that only those dislocations located about the crack front in x_1 – interval $[c - \delta c\ ,\ c]$ will contribute significantly to the stress at $x_1 = c + s$ ahead of the crack tip as s tends to zero ; any other contribution will be negligible for a sufficiently small value of s. We observe that this formula is precise with no place for any other kind of additional stress term. Because x_2 is close to h, we can consider the Taylor series expansion of $\sigma_{ij}^{(J)}(x_1 - x_1', x_2, x_3)$ in (39) about $x_2 = h(x_1)$ to first order with respect to $(x_2 - h)$; this gives

$$\sigma_{ij}^{(J)}(x_1 - x_1', x_2, x_3) = \sigma_{ij}^{(J)}(x_1 - x_1', h, x_3) + \frac{\partial \sigma_{ij}^{(J)}}{\partial x_2}(x_2 - h) + o(x_2 - h) \tag{40}$$

where $o(x_2 - h)$ is the complementary part of the series. Applying the Taylor expansion (40), in $\sigma_{ij}^{(J)}(x_1 - x_1', h(x_1), x_3)$ and $\partial \sigma_{ij}^{(J)} / \partial x_2$ (in which $x_1 = c + s$), appears the difference $(h(x_1) - h(x_1'))$ which we express as follows since x_1 and x_1' (see (39)) are close to c : $h(x_1) = h(c) + p(x_1 - c) + o(x_1 - c)$ and $h(x_1') = h(c) + p(x_1' - c) + o(x_1' - c)$ where $p = \partial h(c) / \partial x_1$; therefore $h(x_1) - h(x_1') = p(x_1 - x_1') + o(x_1 - x_1')$. Furthermore in $\sigma_{ij}^{(C)}$ (39) we restrict ourselves to singularities of the type $s^{-1/2}$ only; this is the singularity that comes into play in the study of planar cracks and gives a well-defined value to the crack extension force. This corresponds to identify $\sigma_{ij}^{(J)}$ to the unbounded terms with $1/(c+s-x_1')$ in the Taylor expansion (40). Assuming $\xi(x_1,x_3)$ and its spatial derivatives with respect to x_3 be bounded at $x_1=c$, the involved integrals in (39) are of the type $\int D_J(x_1')/(c+s-x_1')dx_1'$ which is calculated approximately taking for D_J the straight edge and screw dislocation distributions (35) corresponding to a planar crack π_0 with a straight front parallel to x_3 ***(Figure 3a)***. We obtain ($\sigma_{ij}^{(C)} \equiv \sigma_{ij}^{(C)(I)} + \sigma_{ij}^{(C)(II)} + \sigma_{ij}^{(C)(III)}$):

$$\sigma_{ij}^{(C)(J)} = \left(\tilde{\sigma}_{ij}^{(J)(0)} + \tilde{\sigma}_{ij}^{(J)\xi} + (x_2 - h(c)) \left\{ \frac{\partial \tilde{\sigma}_{ij}^{(J)(0)}}{\partial x_2} + \frac{\partial \tilde{\sigma}_{ij}^{(J)\xi}}{\partial x_2} \right\} \right) \frac{d_J K_J^{(0)}}{C_0^{(J)} \sqrt{2\pi s}} \tag{41}$$

$$K_J^{(0)} = \sqrt{\pi c}\left(\sigma_{22}^a \delta_{JI} + \sigma_{21}^a \delta_{JII} + \sigma_{23}^a \delta_{JIII} \right).$$

In (41), x_2 is close to *h(c)*, this means that $(x_2\text{-}h)$ remains small; the various quantities associated with stresses are given in the Appendix.

III-6. Crack extension force

The crack extension force *G* per unit length of the crack front is calculated in the same way as in [5]. We defined a reduced crack extension force $\tilde{G}$ as

$$\tilde{G} = G / \left(G_0^{(I)} + G_0^{(II)} + G_0^{(III)} \right); \qquad G_0^{(J)} = \frac{b K_J^{(0)^2}}{4\pi C_0^{(J)}} \tag{42}$$

$G_0^{(J)}$ is the crack extension force per unit edge length for planar straight-fronted cracks in Ox_1x_3, extending steadily from $x_1 = -c$ to *c*, under pure mode *J* loading. We obtain the reduced crack extension force at P_c ($x_1 = c$, $x_2 = f$, x_3) as (with $M_{12} \equiv \sigma_{12}^a / \sigma_{22}^a$, $M_{13} \equiv \sigma_{23}^a / \sigma_{22}^a$, $M_{23} \equiv \sigma_{23}^a / \sigma_{21}^a$)

$$\tilde{G}(P_c) = \sum_{i,j=1}^{3} \tilde{G}_j^{(i)}(P_c) \tag{43}$$

$$\tilde{G}_1^{(1)} = -\frac{\partial f(c, x_3)/\partial x_1}{\sqrt{1+(\partial f/\partial x_1)^2+(\partial f/\partial x_3)^2}} \sum_{J=I}^{III}\left(\tilde{\sigma}_{11}^{(J)(0)} + \tilde{\sigma}_{11}^{(J)\xi} + \xi \left\{ \frac{\partial \tilde{\sigma}_{11}^{(J)(0)}}{\partial x_2} + \frac{\partial \tilde{\sigma}_{11}^{(J)\xi}}{\partial x_2} \right\}\right) \frac{d_J K_J^{(0)} d_{II} C_0^{(I)} M_{12}^2}{C_0^{(J)} K_{II}^{(0)} C_0^{(II)} \Delta_{123}},$$

$$\tilde{G}_2^{(1)} = \frac{1}{\sqrt{1+(\partial f/\partial x_1)^2+(\partial f/\partial x_3)^2}} \sum_{J=I}^{III}\left(\tilde{\sigma}_{12}^{(J)(0)} + \tilde{\sigma}_{12}^{(J)\xi} + \xi \left\{ \frac{\partial \tilde{\sigma}_{12}^{(J)(0)}}{\partial x_2} + \frac{\partial \tilde{\sigma}_{12}^{(J)\xi}}{\partial x_2} \right\}\right) \frac{d_J K_J^{(0)} d_{II} C_0^{(I)} M_{12}^2}{C_0^{(J)} K_{II}^{(0)} C_0^{(II)} \Delta_{123}},$$

$$\tilde{G}_3^{(1)} = -\frac{\partial f/\partial x_3}{\sqrt{1+(\partial f/\partial x_1)^2+(\partial f/\partial x_3)^2}} \sum_{J=I}^{III}\left(\tilde{\sigma}_{13}^{(J)(0)} + \tilde{\sigma}_{13}^{(J)\xi} + \xi \left\{ \frac{\partial \tilde{\sigma}_{13}^{(J)(0)}}{\partial x_2} + \frac{\partial \tilde{\sigma}_{13}^{(J)\xi}}{\partial x_2} \right\}\right) \frac{d_J K_J^{(0)} d_{II} C_0^{(I)} M_{12}^2}{C_0^{(J)} K_{II}^{(0)} C_0^{(II)} \Delta_{123}},$$

$$\tilde{G}_1^{(2)} \equiv -\frac{\partial f}{\partial x_1} \frac{d_I C_0^{(II)}}{d_{II} C_0^{(I)} M_{12}} \tilde{G}_2^{(1)},$$

$$\tilde{G}_2^{(2)} = \frac{1}{\sqrt{1+(\partial f/\partial x_1)^2+(\partial f/\partial x_3)^2}} \sum_{J=I}^{III}\left(\tilde{\sigma}_{22}^{(J)(0)} + \tilde{\sigma}_{22}^{(J)\xi} + \xi \left\{ \frac{\partial \tilde{\sigma}_{22}^{(J)(0)}}{\partial x_2} + \frac{\partial \tilde{\sigma}_{22}^{(J)\xi}}{\partial x_2} \right\}\right) \frac{d_J K_J^{(0)} d_I}{C_0^{(J)} K_I^{(0)} \Delta_{123}},$$

$$\tilde{G}_3^{(2)} = -\frac{\partial f/\partial x_3}{\sqrt{1+(\partial f/\partial x_1)^2+(\partial f/\partial x_3)^2}} \sum_{J=I}^{III}\left(\tilde{\sigma}_{23}^{(J)(0)} + \tilde{\sigma}_{23}^{(J)\xi} + \xi \left\{ \frac{\partial \tilde{\sigma}_{23}^{(J)(0)}}{\partial x_2} + \frac{\partial \tilde{\sigma}_{23}^{(J)\xi}}{\partial x_2} \right\}\right) \frac{d_J K_J^{(0)} d_I}{C_0^{(J)} K_I^{(0)} \Delta_{123}},$$

$$\tilde{G}_1^{(3)} \equiv \frac{\partial f/\partial x_1}{\partial f/\partial x_3} \frac{d_{III} C_0^{(II)} M_{13}}{d_{II} C_0^{(III)} M_{12}} \tilde{G}_3^{(1)}, \quad \tilde{G}_2^{(3)} \equiv -\frac{1}{\partial f/\partial x_3} \frac{d_{III} C_0^{(I)} M_{13}}{d_I C_0^{(III)}} \tilde{G}_3^{(2)},$$

$$\tilde{G}_3^{(3)} = -\frac{\partial f/\partial x_3}{\sqrt{1+(\partial f/\partial x_1)^2+(\partial f/\partial x_3)^2}} \sum_{J=I}^{III}\left(\tilde{\sigma}_{33}^{(J)(0)} + \tilde{\sigma}_{33}^{(J)\xi} + \xi \left\{ \frac{\partial \tilde{\sigma}_{33}^{(J)(0)}}{\partial x_2} + \frac{\partial \tilde{\sigma}_{33}^{(J)\xi}}{\partial x_2} \right\}\right) \frac{d_J K_J^{(0)} d_{III} C_0^{(I)} M_{13}^2}{C_0^{(J)} K_{III}^{(0)} C_0^{(III)} \Delta_{123}} \quad (44)$$

$$\Delta_{123} \equiv 1 + (C_0^{(I)} / C_0^{(II)}) M_{12}^2 + (C_0^{(I)} / C_0^{(III)}) M_{13}^2 .$$

Here, quantities associated with stresses are given in the Appendix. In Section 4, we give a more detailed description of G for a special plane-fronted non-planar crack with a segmented front ***(Figure 3c)***.

IV - SPECIAL RESULT : PARTICULAR NON-PLANAR CRACK WITH A SEGMENTED FRONT

The example we shall describe is given in ***Figure 3c***. This is a non-planar crack with a segmented front whose average fracture surface is plane π_0. The crack front at $x_1 = c$ runs indefinitely in the x_3-direction and is in a x_2x_3-plane. We describe ξ below taking locally B as origin. ξ is then odd and $(2\lambda = \lambda_A + \lambda_B)-$periodical with respect to x_3 where λ_A and λ_B ***(Figure 3d)*** are the projected length along x_3 of planar facet A and B respectively. ξ is given by :

$$\begin{aligned} \xi &= \tan\phi_B x_3 , && | x_3 | \le \lambda_B / 2 \\ &= \tan\phi_A (-x_3 + \lambda) , && x_3 \in [\lambda_B / 2,\ \lambda_B / 2 + \lambda_A] . \end{aligned} \tag{45}$$

We assume general loading (mixed mode I+II+III), write $p_0 = p = \tan\theta$ for simplicity in (44) for the reduced crack extension force and express the spatial average $<\tilde{G}>$ of $\tilde{G}$ defined as $<\tilde{G}> = (1/2\lambda)\int_0^{2\lambda} \tilde{G} dx_3$. We obtain

$$<\tilde{G}> = <\tilde{G}^{(1)}> + <\tilde{G}^{(2)}> + <\tilde{G}^{(3)}> ;$$

$$\begin{aligned} <\tilde{G}^{(1)}> = \frac{C_0^{(I)} d_{II} M_{12}}{C_0^{(II)} \Delta_{123}} \Bigg(& \frac{d_{III} M_{13}}{C_0^{(III)}} \left\{ -\tilde{\sigma}_{13}^{(III)(0)} - \frac{2\mu p_0}{1-2\nu} \left[(1-\nu)\hat{u}_{1,1}^{(III)} + \nu \hat{u}_{2,2}^{(III)} + \nu \hat{u}_{3,3}^{(III)} \right] \right. \\ & \left. + \mu \left[\hat{u}_{1,2}^{(III)} + \hat{u}_{2,1}^{(III)} \right] \right\} v_1 - \mu \left\{ \frac{d_I}{C_0^{(I)}} \left(\hat{u}_{1,3}^{(I)} + \hat{u}_{3,1}^{(I)} \right) + \frac{d_{II} M_{12}}{C_0^{(II)}} \left(\hat{u}_{1,3}^{(II)} + \hat{u}_{3,1}^{(II)} \right) \right\} v_2 \\ & + \left\{ \frac{d_I}{C_0^{(I)}} \left(-p_0 \tilde{\sigma}_{11}^{(I)(0)} + \tilde{\sigma}_{12}^{(I)(0)} \right) + \frac{d_{II} M_{12}}{C_0^{(II)}} \left(-p_0 \tilde{\sigma}_{11}^{(II)(0)} + \tilde{\sigma}_{12}^{(II)(0)} \right) \right\} v_0 \Bigg) , \end{aligned}$$

$$<\tilde{G}^{(2)}> = \frac{d_I}{\Delta_{123}} \left(\frac{d_{III} M_{13}}{C_0^{(III)}} \left\{ -\tilde{\sigma}_{23}^{(III)(0)} + \frac{2\mu}{1-2\nu} \left[\nu \hat{u}_{1,1}^{(III)} + (1-\nu)\hat{u}_{2,2}^{(III)} + \nu \hat{u}_{3,3}^{(III)} \right] \right. \right.$$

$$-p_0\mu\left[\hat{u}_{1,2}^{(III)}+\hat{u}_{2,1}^{(III)}\right]\Big\}v_1-\mu\left\{\frac{d_I}{C_0^{(I)}}\left(\hat{u}_{2,3}^{(I)}+\hat{u}_{3,2}^{(I)}\right)+\frac{d_{II}M_{12}}{C_0^{(II)}}\left(\hat{u}_{2,3}^{(II)}+\hat{u}_{3,2}^{(II)}\right)\right\}v_2$$

$$+\left\{\frac{d_I}{C_0^{(I)}}\left(-p_0\tilde{\sigma}_{12}^{(I)(0)}+\tilde{\sigma}_{22}^{(I)(0)}\right)+\frac{d_{II}M_{12}}{C_0^{(II)}}\left(-p_0\tilde{\sigma}_{21}^{(II)(0)}+\tilde{\sigma}_{22}^{(II)(0)}\right)\right\}v_0\Bigg),$$

$$<\tilde{G}^{(3)}>=\frac{d_{III}C_0^{(I)}M_{13}}{C_0^{(III)}\Delta_{123}}\Bigg(-\frac{d_{III}M_{13}2\mu}{C_0^{(III)}(1-2\nu)}\left\{\nu\hat{u}_{1,1}^{(III)}+\nu\hat{u}_{2,2}^{(III)}+(1-\nu)\hat{u}_{3,3}^{(III)}\right\}v_2$$

$$+\Bigg\{\frac{d_I}{C_0^{(I)}}\left(-\mu p_0\left[\hat{u}_{1,3}^{(I)}+\hat{u}_{3,1}^{(I)}\right]+\mu\left[\hat{u}_{2,3}^{(I)}+\hat{u}_{3,2}^{(I)}\right]-\tilde{\sigma}_{33}^{(I)(0)}\right)+\frac{d_{II}M_{12}}{C_0^{(II)}}\Bigg(-\mu p_0\left[\hat{u}_{1,3}^{(II)}+\hat{u}_{3,1}^{(II)}\right]$$

$$+\mu\left[\hat{u}_{2,3}^{(II)}+\hat{u}_{3,2}^{(II)}\right]-\tilde{\sigma}_{33}^{(II)(0)}\Bigg)\Bigg\}v_1+\frac{d_{III}M_{13}}{C_0^{(III)}}\left\{-p_0\tilde{\sigma}_{13}^{(III)(0)}+\tilde{\sigma}_{23}^{(III)(0)}\right\}v_0\Bigg) \tag{46}$$

$$v_0=\left(1/(p_A+p_B)\right)\left(p_A/\sqrt{1+p^2+p_B^2}+p_B/\sqrt{1+p^2+p_A^2}\right),$$
$$v_1=\left(p_Ap_B/(p_A+p_B)\right)\left(-1/\sqrt{1+p^2+p_A^2}+1/\sqrt{1+p^2+p_B^2}\right),$$
$$v_2=\left(p_Ap_B/(p_A+p_B)\right)\left(p_A/\sqrt{1+p^2+p_A^2}+p_B/\sqrt{1+p^2+p_B^2}\right) \tag{47}$$

and $p_A=\tan\phi_A$, $p_B=\tan\phi_B$. Quantities associated to stresses and displacements are given in the Appendix. Hence $<\tilde{G}>$ is a function of parameters $(\tilde{v}_t;p,p_A,p_B;M_{12},M_{13})$ including Poisson's ratio ν ; expressions with Poisson's ratio ν_A originate from normal induced stresses due to Poisson's effect as indicated earlier (Section 2). For $\tilde{v}_t=0$, the static case ([4-6] for example) is recovered; as also are the particular cases of Ox_1x_3-plane moving cracks in pure modes of loading *I*, *II* and *III* [10].When ϕ_B (or ϕ_A) equals zero, the crack front is essentially straight parallel to the x_3-direction. The corresponding crack is like planar crack π_0 ***(Figure 3a)***. First, we look for non-planar cracks for which $<\tilde{G}>$ is larger than 1. Such crack configurations have been found in the quasi-static analyses [4 - 6]. They are expected to be fracture paths in broken real materials. For 0< $<\tilde{G}>$ <1, planar cracks are favoured. Negative values suggest that crack motion is impeded : in the case of planar cracks, we have indicated that the relative displacement of the faces of the crack, formed under load, cancels when motion starts [10]. ***Figure 4*** shows $<\tilde{G}>$ (46) for non-planar cracks travelling at $\tilde{v}_t=0.3$ (ϕ_B= 70°, M_{12}=M_{13}= 10^{-4}).

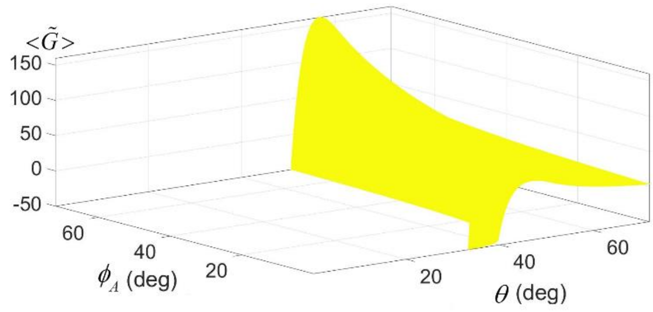

Figure 4 : *Surface* $<\tilde{G}>(\phi_A, \theta)$ *(46) for non-planar cracks moving at* $\tilde{v}_t = 0.3$ *;* $\phi_B = 70°$, $M_{12} = M_{13} = 10^{-4}$, $\nu = 0.22 = \nu_A$, $\beta_{13(t)} = P_t$

Positive values of $<\tilde{G}>$ are observed in a restricted zone of θ (40°< θ <70°, approximately), with a peak in the vicinity of θ =50°; this peak increases continuously with ϕ_A to reach values $<\tilde{G}>\approx 150$ at $\phi_A \approx 70°$.

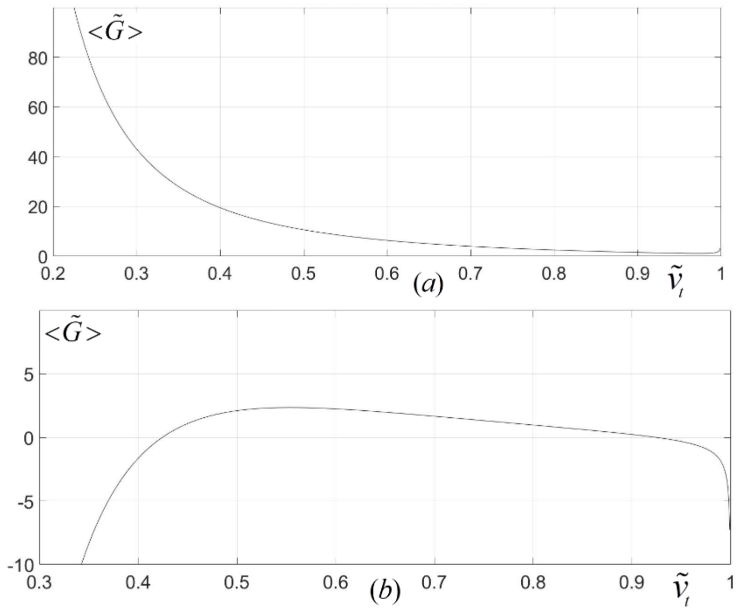

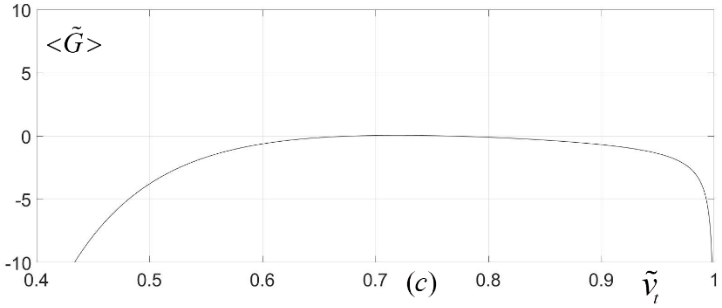

Figure 5 : $<\tilde{G}>$ *(46) as a function of* $\tilde{v}_t$ *for (a)* $\theta = 55°$, *(b)* $\theta = 54°$ *and (c)* $\theta = 53.5°$ *with identical values of the other parameters (*$\phi_A = \phi_B = 70°$, $M_{12} = M_{13} = 10^{-3}$, *ν=1/3=ν*$_A$*). A dramatic change in the form of the curves is observed for a small variation 1° of* θ

***Figure* 5** (*(a)* $\theta = 55°$, *(b)* $\theta = 54°$ and *(c)* $\theta = 53.5°$) shows a non-planar crack whose front is strongly segmented ($\phi_A = \phi_B = 70°$) under dominant mode *I* loading ($M_{12} = M_{13} = 10^{-3}$). When the crack is inclined with respect to Ox_1x_3 by $\theta = 53.5°$ in *(c)*, $<\tilde{G}>$ remains negative for practically all velocity. For a small increase of θ (1.5°), $<\tilde{G}>$ becomes largely positive over a wide range of speed $0.2 \leq \tilde{v}_t \leq 1$ in *(a)*. In *(b)*, a maximum of $<\tilde{G}>$ is present at about $\tilde{v}_t = 0.55 \equiv \tilde{v}_1^{(e)}$; at that velocity, the motion of the crack is uniform along x_1(steady motion). This result is a theoretical prediction of a steady motion for this non-planar crack in solids.

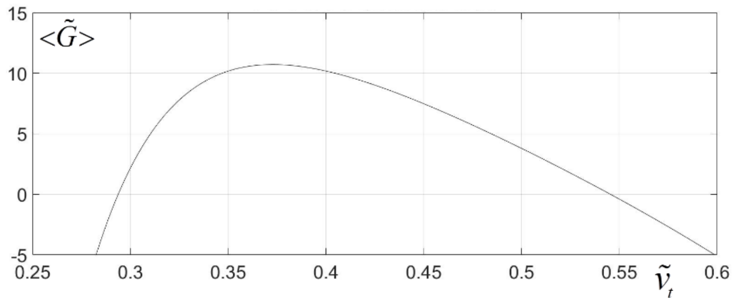

Figure 6 : *Normalized crack extension force* $<\tilde{G}>(\tilde{v}_t)$ *(46) averaged over the length of the segmented crack-front under dominant mode I loading (*$M_{12} = M_{13} = 10^{-4}$*). The average inclination angle with respect to* Ox_1x_3 *is* $\theta_0 = 35°$. *The crack face is almost flat (*$\phi_A = 0.1°; \phi_B = 88°$*); ν=0.22=ν*$_A$*;* $\beta_{13(t)} = P_t$. $\beta_{13(t)} = 1$ *leaves this curve unchanged*

Figure* 6** corresponds to a rather flat crack ($\phi_A = 0.1°$; λ_A large) but with pronounced isolated kinks ($\phi_B = 88°$; λ_B small) (for λ_A and λ_B, see ***Figure 3d). The average inclination angle of the crack with respect to Ox_1x_3 is $\theta = 35°$. Mode I loading is dominant ($M_{12} = M_{13} = 10^{-4}$). $< \tilde{G} >$ is largely above 1 in $0.3 \leq \tilde{v}_t \leq 0.55$, approximately. Interestingly, we have checked that $\beta_{13(t)} = 1$ leaves unchanged this curve.

V - DISCUSSION

The determination of the elastic fields of dislocations in motion may be performed by two general methods called "Method of Fourier series or integrals" and "Method of Green's functions" in review works by Mura [8, 9]. The first method, especially powerful for many cases, is the one adopted in the present study (Section 2.1); it has been used to obtain the elastic fields of a dislocation oscillating in the form of a standing wave [3], for example. The dislocation elastic fields measured by an observer in an inertial reference frame moving with the dislocation, are like those of a static dislocation in the laboratory, particularly in the subsonic regime. This allows to describe static and uniformly moving cracks in a similar way. Hence, there is one-one similarity in form (in both cases) of crack characteristic quantities: crack dislocation distributions D_J (35) and corresponding relative displacements of the faces of the crack ϕ_J (37), stresses at the tip of the crack $\sigma_{ij}^{(C)(J)}$ (41) and crack extension force G (42- 44); for the static case, we may refer to [5] and references therein.

Most theoretical analyses in fracture mechanics concern planar cracks, with straight fronts, in static position or in uniform movement (see ***Figure 3a*** for illustration). Because the length of the crack front is large in general, the modelling applies in practice to cracking over large distances. Crack propagation is the mechanism controlling fracture with no place for nucleation. For non-planar cracks, the modelling extends to flat-fronted cracks. The crack front f (1) is arbitrary (see ***Figure 1***); a simple special case is given in ***Figure 3c***. For these non-planar cracks, most of the work refers to the static case. The present study is a first extension to the uniform motion of the x_2x_3-plane front of the crack; the static case is restored when $v = 0$. The numerical application (Section 4) here concerns a front made up of 2 types of inclined segments, with angles ϕ_A and ϕ_B, with respect to the x_3-direction ***(Figure 3c, d)***. On average, the crack fluctuates around the plane π_0 ***(Figure 3a)*** inclined by $\theta = \theta_0$ with respect to Ox_1x_3 with Ox_3 as the axis of rotation. When the crack front is strongly segmented ($\phi_A = \phi_B$ large) as in ***Figure 5***, the highest positive values of $< \tilde{G} >$

(46) are for θ> 53.5° in dominant mode I loading. A maximum of $<\tilde{G}>$, $<\tilde{G}>_{\max 1} \cong 2.5$, is observed for $\tilde{v}_t = 0.55 \equiv \tilde{v}_1^{(e)}$ with $\theta = 54°$ ***(Figure 5b)***. For the moving planar crack in Ox_1x_3, the steady motion velocity found is at $\tilde{v}_t = 0.52$ for ν= 1/3 [10]. We may safely say that, for the crack corresponding to ***Figure 5***, the steady motion is predicted at the velocity $\tilde{v}_1^{(e)}$. A second example (in dominant mode *I* loading and $\theta = 35°$) where the crack front is flat over large distance λ_A ($\phi_A = 0.1°$) with isolated kinks strongly inclined ($\phi_B = 88°$) over short distance λ_B is also presented ***(Figure 6)***. The velocity interval where $<\tilde{G}>$ is positive and larger than 1 is $\tilde{v}_t \in [0.3,\ 0.54]$, approximately. Out of that interval, the motion of the crack is not favoured. A maximum of $<\tilde{G}>$, $<\tilde{G}>_{\max 2} \cong 11.2$, is observed at $\tilde{v}_t = 0.37 \equiv \tilde{v}_2^{(e)}$. We can also safely say this is the steady motion condition. We shall use ***Figure 6*** to provide a qualitative explanation of crack branching observed in glass. ***Figure 7*** shows the broken surface of a glass rod in tension [13]. Fracture propagates from bottom to top from a surface flaw. Initially, the crack is flat and smooth over a relatively large area; then branching occurs. The latter covers a region that is flat on average ($\phi_A \approx 0$) but comprising pronounced short spaced segmentations ($\phi_B \approx 90$ °). The crack progresses upwards with an increasing speed v from zero; for a certain value v_1, it turns into a non-plane crack. The transformation takes place without any attenuation of the speed regime. Using ***Figure 6***, we propose the following explanation: for $\tilde{v}_t < 0.3$, the planar starter crack is favoured; its speed increases towards the terminal velocity.

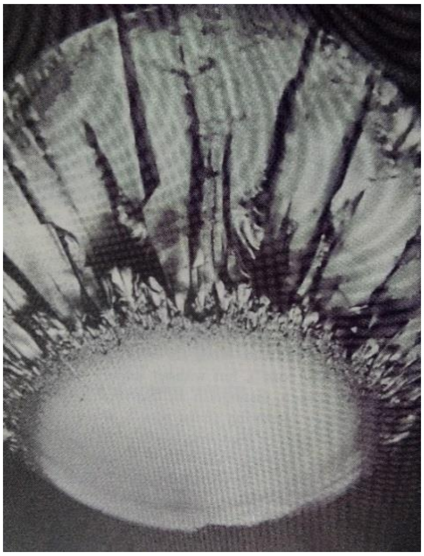

Figure 7 : *Fracture surface of broken rod of glass under tension viewed in optical microscopy. Fracture propagated from bottom to top. Rod diameter 4.5 mm* (*see* [13])

We recall that an estimate of the terminal velocity depending on Poisson's ratio is offered by [10] where it is shown to be about $v^{(e)} \cong 0.52c_t$ for ν= 1/3; it is also shown there that above the terminal velocity, the crack extension force for the tensile planar crack decreases rapidly towards zero. ***Figure 6*** tells us that in the velocity range $\tilde{v}_t \in [0.3,\ 0.54]$ non-planar crack configurations (similar to that observed in ***Figure 7***) exist with a much larger value of the crack extension force. Hence, the starter planar crack transforms itself into a non-planar configuration to maintain its motion.

VI - CONCLUSION

In the present study, non-planar cracks of finite extension in the x_1 and x_2 directions and infinite along x_3, inside an infinitely extended elastic medium, subjected to mixed mode I+II+III loading, have been investigated. The loadings σ_{22}^a, σ_{21}^a and σ_{23}^a are applied along the x_2, x_1 and x_3 directions, respectively. The front of the crack is planar in x_2x_3 and travels at a constant velocity v along the x_1 - direction whilst its faces remain stress free. The crack front has an average elevation $h = h(x_1)$ from Ox_1x_3 and fluctuates weakly about that position in the form $\xi = \xi(x_1,\ x_3)$ (1). The crack is represented by a continuous distribution of 3 types J (J=I, II and III) of infinitesimal dislocation having the shape of the crack front. The associated Burgers vectors $\vec{b}_I = (0,b,0)$, $\vec{b}_{II} = (b,0,0)$ and $\vec{b}_{III} = (0,0,b)$ are directed along the applied loadings, tension and shears directions, respectively. Adopting the method of Fourier series [8, 9] (Section 2.1), we give explicit expression of the elastic fields (displacement and stress) of the dislocations J (Sections 3.1 to 3.3). Then, distribution functions D_J of straight dislocation arrays corresponding to a planar crack π_0, inclined by angle θ_0 with respect to Ox_1x_3 are calculated (Section 3.4). Adopting these D_J, we propose explicit expressions of the crack-tip stresses (Section 3.5) and crack extension force per unit length of the crack front (Section 3.6) for the general form f (1). The analysis is then applied to a simple special non-planar crack with a segmented front (Section 4). This type of crack is given on ***Figure* 3*c, d***; the average surface is plane π_0 ***(Figure 3a)*** ; its front is segmented, at the average elevation $h(x_1)$ from Ox_1x_3 in the x_2x_3 located at x_1, in the form (45). We distinguish two types of segmentation characterized by angles ϕ_A and ϕ_B of the segments with respect to x_3 direction. We show first that for this type of special cracks, configurations exist for which values $\langle G \rangle$, averaged over the length of the crack front, are larger than those corresponding to the planar crack travelling in Ox_1x_3 ***(Figure 4)*** in similar velocity intervals. Then, two types of segmentation are investigated under dominant mode I loading : (1) Strong segmentation of the crack front

($\phi_A = \phi_B = 70°$), ***Figure 5***. We show that a steady motion sets in at the velocity $v_1^{(e)} = 0.55c_t$ for an inclination $\theta = 54°$. (2) Weak segmentation, flat average fracture surface with isolated strong kinks (ϕ_A= 0.1°, ϕ_B= 88°). A steady motion is also evidenced at the velocity $v_2^{(e)} = 0.37c_t$ when $\theta = 35°$. The latter configuration ***(Figure 6)*** explains crack branching observed in the fracture of glass.

REFERENCES

[1] - P. N. B. ANONGBA, A non-planar crack analysis using continuously distributed sinusoidal edge dislocations and linear elasticity, *Physica Stat. Sol. B*, 194 (1996) 443 - 452

[2] - P. N. B. ANONGBA and V. VITEK, Significance of the deviations of the crack front into the plane perpendicular to the crack propagation direction : I. Crack-front dislocation generation, *Int. J. Fract.*, 124 (2003) 1 - 15

[3] - P. N. B. ANONGBA, Significance of the deviations of the crack front into the plane perpendicular to the crack propagation direction : II. Crack-front vibration, *Int. J. Fract.*, 124 (2003) 17 - 31

[4] - P. N. B. ANONGBA, A study of the mixed mode I+III loading of a non-planar crack using infinitesimal dislocations, *Rev. Ivoir. Sci. Technol.*, 14 (2009) 55 - 86

[5] - P. N. B. ANONGBA, Non-planar crack under general loading : dislocation, crack-tip stress and crack extension force, *Rev. Ivoir. Sci. Technol.*, 16 (2010) 11 - 50

[6] - P. N. B. ANONGBA, Non-planar crack under general loading and induced normal stresses due to Poisson effect, *Rev. Ivoir. Sci. Technol.*, 30 (2017) 37 - 57

[7] - P. N. B. ANONGBA, Non-planar interface crack under general loading : III. Dislocation, crack-tip stress and crack extension force, *Rev. Ivoir. Sci. Technol.*, 32 (2018) 10 - 47

[8] - T. MURA, The continuum theory of dislocations, In : "Advances in Materials Research" (Edited by H. Herman), *Interscience Publications*, Vol. 3, (1968) 1 - 108

[9] - T. MURA, "Micromechanics of defects in Solids", Martinus Nijhoff Publishers, Dordrecht, (1987)

[10] - P. N. B. ANONGBA, Planar cracks in uniform motion under mode I and II loadings, *Rev. Ivoir. Sci. Technol.*, 35 (2020) 1 - 22

[11] - B. A. BILBY and J. D. ESHELBY, Dislocations and the theory of fracture, In : "Fracture", Ed. Academic Press (H. Liebowitz), New York, Vol. 1, (1968) 99 - 182

[12] - J. D. ESHELBY, Aspects of the theory of dislocations, In: "Mechanics of solids : The Rodney Hill 60th Anniversary Volume", Ed. Pergamon Press (H.G. Hopkins and M.J. Sewell), *Oxford*, (1982) 185 - 225

[13] - J. W. JOHNSON and D. G. HOLLOWAY, On the shape and size of the fracture zones on glass fracture surfaces, *Phil. Mag.*, 14 (1966) 731 - 743

APPENDIX

The various quantities involve in the stresses at the tip of the crack (41) and crack extension force G (44), Section 3, are given in the following. For terms with the superscript ξ in (41), similar relations as in (28) between stress and displacement are used here (J= I, II and III) :

$$\tilde{\sigma}_{ii}^{(J)\xi}=\frac{2\mu}{1-2\nu}\Big(\big[\delta_{i1}(1-\nu)+\nu(\delta_{i2}+\delta_{i3})\big]\tilde{u}_{1,1}^{(J)\xi}+\big[\delta_{i2}(1-\nu)+\nu(\delta_{i1}+\delta_{i3})\big]\tilde{u}_{2,2}^{(J)\xi}$$
$$+\big[\delta_{i3}(1-\nu)+\nu(\delta_{i1}+\delta_{i2})\big]\tilde{u}_{3,3}^{(J)\xi}\Big),$$
$$\frac{\partial\tilde{\sigma}_{ii}^{(J)\xi}}{\partial x_2}=\frac{2\mu}{1-2\nu}\Big(\big[\delta_{i1}(1-\nu)+\nu(\delta_{i2}+\delta_{i3})\big]\tilde{u}_{1,21}^{(J)\xi}+\big[\delta_{i2}(1-\nu)+\nu(\delta_{i1}+\delta_{i3})\big]\tilde{u}_{2,22}^{(J)\xi}$$
$$+\big[\delta_{i3}(1-\nu)+\nu(\delta_{i1}+\delta_{i2})\big]\tilde{u}_{3,23}^{(J)\xi}\Big),\ i=1,\ 2\text{ and }3\ ;$$

$$\tilde{\sigma}_{ij}^{(J)\xi}=\mu\left(\tilde{u}_{i,j}^{(J)\xi}+\tilde{u}_{j,i}^{(J)\xi}\right),$$
$$\partial\tilde{\sigma}_{ij}^{(J)\xi}/\partial x_2=\mu\left(\tilde{u}_{i,2j}^{(J)\xi}+\tilde{u}_{j,2i}^{(J)\xi}\right),\quad i\neq j \tag{A.1}$$

For J=I, II and III, we listed below the various quantities associated to the displacements in (A.1).
For J= I :

$$\tilde{\sigma}_{11}^{(I)(0)}=\frac{\mu b}{\pi\tilde{v}_t^2}\left(\frac{2+(1-2c_*^2)\tilde{v}_t^2}{P_l[1+p^2P_l^2]}-\frac{2P_{2t}^2}{P_t[1+p^2P_t^2]}\right),$$
$$\tilde{\sigma}_{22}^{(I)(0)}=\frac{2\mu bP_{2t}^2}{\pi\tilde{v}_t^2}\left(\frac{1}{P_t[1+p^2P_t^2]}-\frac{1}{P_l[1+p^2P_l^2]}\right),\qquad \tilde{\sigma}_{33}^{(I)(0)}=\frac{\mu b(1-2c_*^2)}{\pi P_l[1+p^2P_l^2]};$$
$$\partial\tilde{\sigma}_{ii}^{(I)(0)}/\partial x_2=0,\quad i=1,\ 2\text{ and }3;$$
$$\tilde{\sigma}_{21}^{(I)(0)}=\frac{2\mu bp}{\pi\tilde{v}_t^2}\left(\frac{P_l}{1+p^2P_l^2}-\frac{P_{2t}^4}{P_t[1+p^2P_t^2]}\right),\quad \partial\tilde{\sigma}_{21}^{(I)(0)}/\partial x_2=0;$$
$$\tilde{\sigma}_{j3}^{(I)(0)}=0,\quad \partial\tilde{\sigma}_{j3}^{(I)(0)}/\partial x_2=0,\qquad j=1\text{ and }2 \tag{A.2}$$

$$\tilde{u}_{i,i}^{(I)\xi}=0,\quad i=1,\ 2\text{ and }3;$$
$$\tilde{u}_{1,21}^{(I)\xi}=-\frac{b}{\pi\tilde{v}_t^2}\left(\frac{p_{2t}^2[1-p^2P_t^2]}{2P_t[1+p^2P_t^2]^2}-\frac{(1-\nu)c_*^2[1-p^2P_l^2]}{(1-2\nu)P_l[1+p^2P_l^2]^2}\right)\frac{\partial^2\xi(c,x_3)}{\partial x_3^2}\equiv\hat{u}_{1,21}^{(I)}\frac{\partial^2\xi}{\partial x_3^2},$$
$$\tilde{u}_{2,22}^{(I)\xi}=-\frac{b}{2\pi\tilde{v}_t^2}\left(\frac{\tilde{v}_t^2[5+3p^2P_t^2]-2[3+p^2P_t^2]}{2P_t[1+p^2P_t^2]^2}\right.$$

$$+\frac{2(1-\nu)c_*^2P_l[3+p^2P_l^2]}{(1-2\nu)[1+p^2P_l^2]^2}\Bigg)\frac{\partial^2\xi}{\partial x_3^2}\equiv\hat{u}_{2,22}^{(I)}\frac{\partial^2\xi}{\partial x_3^2},$$

$$\tilde{u}_{3,23}^{(I)\xi}=\frac{b(c_*^{-2}-1)}{\pi\tilde{v}_t^2}\left(\frac{2(1-\nu)c_*^2P_l}{1+p^2P_l^2}-\frac{(1-2\nu)P_t}{1+p^2P_t^2}\right)\frac{\partial^2\xi}{\partial x_3^2}\equiv\hat{u}_{3,23}^{(I)}\frac{\partial^2\xi}{\partial x_3^2};$$

$$\tilde{u}_{3,2}^{(I)\xi}=\frac{b(c_*^{-2}-1)}{\pi\tilde{v}_t^2}\left(\frac{2(1-\nu)c_*^2P_l}{1+p^2P_l^2}-\frac{(1-2\nu)P_t}{1+p^2P_t^2}\right)\frac{\partial\xi}{\partial x_3}\equiv\hat{u}_{3,2}^{(I)}\frac{\partial\xi}{\partial x_3},\qquad \tilde{u}_{3,22}^{(I)\xi}=0;$$

$$\tilde{u}_{2,3}^{(I)\xi}=\frac{b}{\pi\tilde{v}_t^2}\left(\frac{2(1-\nu)c_*^2P_l}{(1-2\nu)[1+p^2P_l^2]}-\frac{P_{2t}^2}{P_t[1+p^2P_t^2]}\right)\frac{\partial\xi}{\partial x_3}\equiv\hat{u}_{2,3}^{(I)}\frac{\partial\xi}{\partial x_3},\qquad \tilde{u}_{2,23}^{(I)\xi}=0;$$

$$\tilde{u}_{1,2}^{(I)\xi}=0,\quad \tilde{u}_{1,22}^{(I)\xi}=\frac{bp}{2\pi\tilde{v}_t^2}\Bigg(\frac{2(1-\nu)c_*^2P_l[3+p^2P_l^2]}{(1-2\nu)[1+p^2P_l^2]^2}$$

$$-\frac{P_{2t}^2P_t[3+p^2P_t^2]}{[1+p^2P_t^2]^2}\Bigg)\frac{\partial^2\xi}{\partial x_3^2}\equiv\hat{u}_{1,22}^{(I)}\frac{\partial^2\xi}{\partial x_3^2};$$

$$\tilde{u}_{2,1}^{(I)\xi}=0,\quad \tilde{u}_{2,21}^{(I)\xi}=\frac{bp}{4\pi\tilde{v}_t^2}\Bigg(\frac{4(1-\nu)c_*^2P_l[3+p^2(1-3\tilde{v}_l^2)]}{(1-2\nu)[1+p^2P_l^2]^2}$$

$$-\frac{6-5\tilde{v}_t^2+p^2P_t^2[2-7\tilde{v}_t^2]}{P_t[1+p^2P_t^2]^2}\Bigg)\frac{\partial^2\xi}{\partial x_3^2}\equiv\hat{u}_{2,21}^{(I)}\frac{\partial^2\xi}{\partial x_3^2};$$

$$\tilde{u}_{1,3}^{(I)\xi}=\frac{bp}{\pi\tilde{v}_t^2}\left(\frac{P_{2t}^2P_t}{1+p^2P_t^2}-\frac{2(1-\nu)c_*^2P_l}{(1-2\nu)[1+p^2P_l^2]}\right)\frac{\partial\xi}{\partial x_3}\equiv\hat{u}_{1,3}^{(I)}\frac{\partial\xi}{\partial x_3},\qquad \tilde{u}_{1,23}^{(I)\xi}=0;$$

$$\tilde{u}_{3,1}^{(I)\xi}=\frac{b(c_*^{-2}-1)p}{\pi\tilde{v}_t^2}\left(\frac{(1-2\nu)P_t}{1+p^2P_t^2}-\frac{2(1-\nu)c_*^2P_l}{1+p^2P_l^2}\right)\frac{\partial\xi}{\partial x_3}\equiv\hat{u}_{3,1}^{(I)}\frac{\partial\xi}{\partial x_3},\quad \tilde{u}_{3,21}^{(I)\xi}=0 \qquad \text{(A.3)}$$

For $J=II$:

$$\tilde{\sigma}_{11}^{(II)(0)}=\frac{\mu bp}{\pi\tilde{v}_t^2}\left(\frac{2P_tP_{2t}^2}{1+p^2P_t^2}+\frac{P_l[(c_*^{-2}-2)P_l^2-c_*^{-2}]}{1+p^2P_l^2}\right),$$

$$\tilde{\sigma}_{22}^{(II)(0)}=\frac{\mu bp}{\pi\tilde{v}_t^2}\left(\frac{P_l[c_*^{-2}P_l^2-c_*^{-2}+2]}{1+p^2P_l^2}-\frac{2P_tP_{2t}^2}{1+p^2P_t^2}\right),\qquad \tilde{\sigma}_{33}^{(II)(0)}=-\frac{\mu b(1-2c_*^2)pP_l}{\pi[1+p^2P_l^2]};$$

$\partial\tilde{\sigma}_{ii}^{(II)(0)}/\partial x_2=0$, i=1, 2 and 3;

$$\tilde{\sigma}_{21}^{(II)(0)}=\frac{2\mu b}{\pi\tilde{v}_t^2}\left(\frac{P_l}{1+p^2P_l^2}-\frac{P_{2t}^4}{P_t[1+p^2P_t^2]}\right),\quad \partial\tilde{\sigma}_{21}^{(II)(0)}/\partial x_2=0 \qquad \text{(A.4)}$$

The other stresses and their derivatives of order zero with respect to ξ corresponding to the straight dislocation are zero. We have

$$\tilde{u}_{i,i}^{(II)\xi} = 0\,, \quad i{=}1,\ 2 \text{ and } 3;$$

$$\tilde{u}_{1,21}^{(II)\xi} = \frac{bp}{2\pi\tilde{v}_t^2}\left(\frac{p_{2t}^2 P_t[1-p^2P_t^2]}{[1+p^2P_t^2]^2} - \frac{2(1-\nu)c_*^2 P_l[1-p^2P_l^2]}{(1-2\nu)[1+p^2P_l^2]^2}\right)\frac{\partial^2\xi(c,x_3)}{\partial x_3^2} \equiv \hat{u}_{1,21}^{(II)}\frac{\partial^2\xi}{\partial x_3^2}\,,$$

$$\tilde{u}_{2,22}^{(II)\xi} = \frac{bp}{2\pi\tilde{v}_t^2}\left(\frac{2(1-\nu)c_*^2 P_l^3[3+p^2P_l^2]}{(1-2\nu)[1+p^2P_l^2]^2}\right.$$
$$\left. - \frac{P_{2t}^2 P_t[3+p^2P_t^2]}{[1+p^2P_t^2]^2}\right)\frac{\partial^2\xi}{\partial x_3^2} \equiv \hat{u}_{2,22}^{(II)}\frac{\partial^2\xi}{\partial x_3^2}\,,$$

$$\tilde{u}_{3,23}^{(II)\xi} = -\frac{bp}{\pi\tilde{v}_t^2}\left(\frac{(1-2\nu)(1-c_*^{-2})P_{2t}^2 P_t}{1+p^2P_t^2} + \frac{2(1-\nu)(1-c_*^2)P_l^3}{1+p^2P_l^2}\right)\frac{\partial^2\xi}{\partial x_3^2} \equiv \hat{u}_{3,23}^{(II)}\frac{\partial^2\xi}{\partial x_3^2}\,;$$

$$\tilde{u}_{1,2}^{(II)\xi} = 0\,, \quad \tilde{u}_{1,22}^{(II)\xi} = \frac{b}{2\pi\tilde{v}_t^2}\left(\frac{2(1-\nu)c_*^2 P_l[1-p^2P_l^2]}{(1-2\nu)[1+p^2P_l^2]^2} - \frac{\tilde{v}_t^2 P_t[(1-2\nu)c_*^{-2} - 2(1-\nu)]}{1+p^2P_t^2}\right.$$
$$\left. - \frac{P_{2t}^2 P_t[1-p^2P_t^2]}{[1+p^2P_t^2]^2}\right)\frac{\partial^2\xi}{\partial x_3^2} \equiv \hat{u}_{1,22}^{(II)}\frac{\partial^2\xi}{\partial x_3^2}\,;$$

$$\tilde{u}_{2,1}^{(II)\xi} = 0\,,\ \tilde{u}_{2,21}^{(II)\xi} = \frac{b}{2\pi\tilde{v}_t^2}\left(\frac{2(1-\nu)c_*^2 P_l[1-p^2P_l^2]}{(1-2\nu)[1+p^2P_l^2]^2} - \frac{P_{2t}^2[1-p^2P_t^2]}{P_t[1+p^2P_t^2]^2}\right)\frac{\partial^2\xi}{\partial x_3^2} \equiv \hat{u}_{2,21}^{(II)}\frac{\partial^2\xi}{\partial x_3^2}\,;$$

$$\tilde{u}_{1,3}^{(II)\xi} = \frac{b}{\pi\tilde{v}_t^2}\left(\frac{P_{2t}^2 P_t}{1+p^2P_t^2} - \frac{2(1-\nu)c_*^2 P_l}{(1-2\nu)][1+p^2P_l^2]}\right)\frac{\partial\xi}{\partial x_3} \equiv \hat{u}_{1,3}^{(II)}\frac{\partial\xi}{\partial x_3}\,, \qquad \tilde{u}_{1,23}^{(II)\xi} = 0\,;$$

$$\tilde{u}_{2,3}^{(II)\xi} = \frac{bp}{\pi\tilde{v}_t^2}\left(\frac{P_{2t}^2 P_t}{1+p^2P_t^2} - \frac{2(1-\nu)c_*^2 P_l^3}{(1-2\nu)[1+p^2P_l^2]}\right)\frac{\partial\xi}{\partial x_3} \equiv \hat{u}_{2,3}^{(II)}\frac{\partial\xi}{\partial x_3}\,, \qquad \tilde{u}_{2,23}^{(II)\xi} = 0\,;$$

$$\tilde{u}_{3,1}^{(II)\xi} = \frac{b}{\pi\tilde{v}_t^2}\left(\frac{(1-2\nu)(c_*^{-2}-1)P_{2t}^2}{P_t[1+p^2P_t^2]} - \frac{2(1-\nu)(1-c_*^2)P_l}{1+p^2P_l^2}\right)\frac{\partial\xi}{\partial x_3} \equiv \hat{u}_{3,1}^{(II)}\frac{\partial\xi}{\partial x_3}\,,\ \tilde{u}_{3,21}^{(II)\xi} = 0\,;$$

$$\tilde{u}_{3,2}^{(II)\xi} = \frac{bp}{\pi\tilde{v}_t^2}\left(\frac{(1-2\nu)(c_*^{-2}-1)P_{2t}^2 P_t}{1+p^2P_t^2} - \frac{2(1-\nu)(1-c_*^2)P_l^3}{1+p^2P_l^2}\right)\frac{\partial\xi}{\partial x_3} \equiv \hat{u}_{3,2}^{(II)}\frac{\partial\xi}{\partial x_3}\,,$$
$$\tilde{u}_{3,22}^{(II)\xi} = 0 \qquad \text{(A.5)}$$

For $J = III$:

$$\tilde{\sigma}_{13}^{(III)(0)} = -\frac{\mu b p P_t}{2\pi\beta_{13(t)}^2[1+p^2P_t^2]}, \qquad \partial\tilde{\sigma}_{13}^{(III)(0)}/\partial x_2 = 0\,;$$

$$\tilde{\sigma}_{23}^{(III)(0)} = \frac{\mu b P_t}{2\pi \beta_{13(t)}^2 [1 + p^2 P_t^2]}, \qquad \partial \tilde{\sigma}_{23}^{(III)(0)} / \partial x_2 = 0 \tag{A.6}$$

All the other similar quantities associated with the stresses, of zero order with respect to ξ, are zero. We have

$$\tilde{u}_{1,1}^{(III)\xi} = \frac{b}{2\pi \tilde{v}_t^2} \left(\frac{2(1-2\nu)(c_*^{-2}-1) - \tilde{v}_t^2}{P_t[1+p^2P_t^2]} - \frac{4(1-\nu)(1-c_*^2)}{P_l[1+p^2P_l^2]} \right) \frac{\partial \xi}{\partial x_3} \equiv \hat{u}_{1,1}^{(III)} \frac{\partial \xi}{\partial x_3},$$

$$\tilde{u}_{2,2}^{(III)\xi} = \frac{b(c_*^{-2}-1)}{\pi \tilde{v}_t^2} \left(\frac{2(1-\nu)c_*^2 P_l}{1+p^2P_l^2} - \frac{(1-2\nu)P_t}{1+p^2P_t^2} \right) \frac{\partial \xi}{\partial x_3} \equiv \hat{u}_{2,2}^{(III)} \frac{\partial \xi}{\partial x_3},$$

$$\tilde{u}_{3,3}^{(III)\xi} = -\frac{b}{2\pi} \frac{1}{P_t[1+p^2P_t^2]} \frac{\partial \xi}{\partial x_3} \equiv \hat{u}_{3,3}^{(III)} \frac{\partial \xi}{\partial x_3}, \qquad \tilde{u}_{i,2i}^{(III)\xi} = 0, \quad i = 1, 2 \text{ and } 3;$$

$$\tilde{u}_{1,2}^{(III)\xi} = \frac{bp}{2\pi \tilde{v}_t^2} \left(\frac{[2(1-2\nu)(c_*^{-2}-1) - \tilde{v}_t^2]P_t}{1+p^2P_t^2} - \frac{4(1-\nu)(1-c_*^2)P_l}{1+p^2P_l^2} \right) \frac{\partial \xi}{\partial x_3} \equiv \hat{u}_{1,2}^{(III)} \frac{\partial \xi}{\partial x_3},$$

$$\tilde{u}_{1,22}^{(III)\xi} = 0;$$

$$\tilde{u}_{2,1}^{(III)\xi} = \frac{b(c_*^{-2}-1)p}{\pi \tilde{v}_t^2} \left(\frac{(1-2\nu)P_t}{1+p^2P_t^2} - \frac{2(1-\nu)c_*^2 P_l}{1+p^2P_l^2} \right) \frac{\partial \xi}{\partial x_3} \equiv \hat{u}_{2,1}^{(III)} \frac{\partial \xi}{\partial x_3}, \qquad \tilde{u}_{2,21}^{(III)\xi} = 0;$$

$$\tilde{u}_{2,23}^{(III)\xi} = \frac{b(c_*^{-2}-1)}{\pi \tilde{v}_t^2} \left(\frac{2(1-\nu)c_*^2 P_l}{1+p^2P_l^2} - \frac{(1-2\nu)P_t}{1+p^2P_t^2} \right) \frac{\partial^2 \xi}{\partial x_3^2} \equiv \hat{u}_{2,23}^{(III)} \frac{\partial^2 \xi}{\partial x_3^2}, \qquad \tilde{u}_{2,3}^{(III)\xi} = 0.$$

$$\tilde{u}_{3,1}^{(III)\xi} = 0, \quad \tilde{u}_{3,21}^{(III)\xi} = \frac{bp}{2\pi} \left(\frac{2(c_*^{-2}-1)}{\tilde{v}_t^2} \left[\frac{(1-2\nu)P_t}{1+p^2P_t^2} - \frac{2(1-\nu)c_*^2 P_l}{1+p^2P_l^2} \right] - \frac{1-p^2P_t^2}{2P_t[1+p^2P_t^2]^2} \right) \frac{\partial^2 \xi}{\partial x_3^2} \equiv \hat{u}_{3,21}^{(III)} \frac{\partial^2 \xi}{\partial x_3^2};$$

$$\tilde{u}_{3,2}^{(III)\xi} = 0, \quad \tilde{u}_{3,22}^{(III)\xi} = \frac{b}{2\pi} \left(\frac{2(c_*^{-2}-1)}{\tilde{v}_t^2} \left[\frac{2(1-\nu)c_*^2 P_l}{1+p^2P_l^2} - \frac{(1-2\nu)P_t}{1+p^2P_t^2} \right] + \frac{1-p^2P_t^2}{2P_t[1+p^2P_t^2]^2} \right) \frac{\partial^2 \xi}{\partial x_3^2} \equiv \hat{u}_{3,22}^{(III)} \frac{\partial^2 \xi}{\partial x_3^2};$$

$$\tilde{u}_{1,23}^{(III)\xi} = \frac{bp}{2\pi \tilde{v}_t^2} \left(\frac{[2(1-2\nu)(c_*^{-2}-1) - \tilde{v}_t^2]P_t}{1+p^2P_t^2} - \frac{4(1-\nu)(1-c_*^2)P_l}{1+p^2P_l^2} \right) \frac{\partial^2 \xi}{\partial x_3^2} \equiv \hat{u}_{1,23}^{(III)} \frac{\partial^2 \xi}{\partial x_3^2},$$

$$\tilde{u}_{1,3}^{(III)\xi} = 0 \tag{A.7}$$